10 EUR

HUNGARIAN GROUP OF *fib*

CONCRETE STRUCTURES

ANNUAL TECHNICAL JOURNAL

2019

Vol. 20

FERROBETON

safe basis provided by concrete

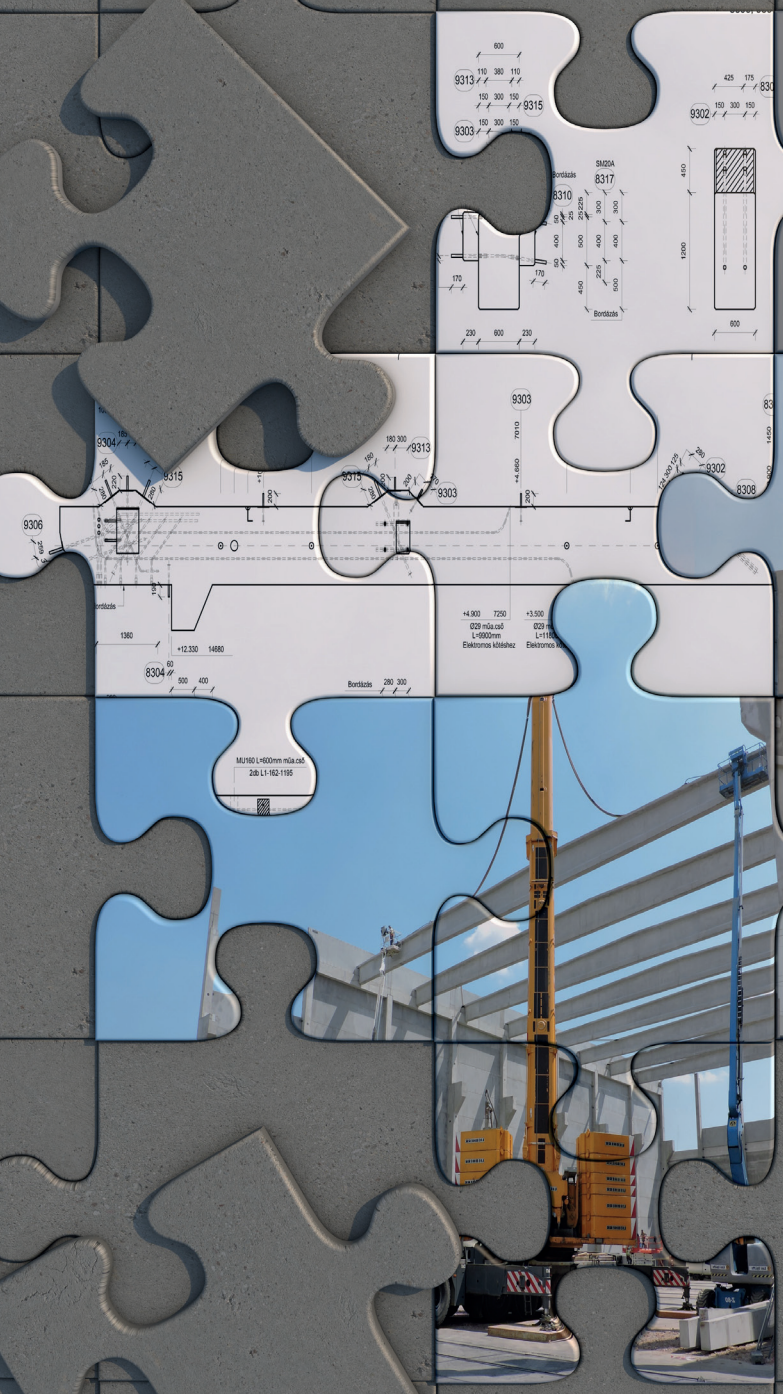

www.ferrobeton.hu

CONCRETE STRUCTURES
Journal of the Hungarian Group of ***fib***

Founded by: Hungarian Group of ***fib***
Publisher: Hungarian Group of ***fib***
(***fib*** = International Federation for Structural Concrete)

Editorial office:
Budapest University of Technology and Economics (BME)
Department of Construction Materials and Engineering Geology
Műegyetem rkp. 3., H-1111 Budapest
Phone: +36-1-463 4068
Fax: +36-1-463 3450
WEB http://www.fib.bme.hu
WEB editor: Dr. Olivér Czoboly

Layout and print: Csaba Halmai, Navigar Ltd.

Price: 10 EUR, Printed in 1000 copies

HU ISSN 2062-7904
online ISSN: 1586-0361

Cover photo:
National Gallery of Australia, Canberra
Photo by György L. Balázs

CONTENT

Sponsors:

Railway Bridges Foundation, ÉMI Nonprofit Ltd., HÍDÉPÍTÕ Co., Holcim Hungary Co., MÁV Co., MSC Consulting Co., Lábatlani Vasbetonipari Co., Pont-*TERV* Co., UVATERV Co., MÉLYÉPTERV KOMPLEX Engineering Co., SW Umwelttechnik Hungary Ltd., Betonmix Consulting Ltd., BVM Épelem Ltd., CAEC Ltd., Pannon Freyssinet Ltd., STABIL PLAN Ltd., UNION PLAN Ltd., DCB Consulting Ltd., BME Dept. of Structural Engineering, BME Dept. of Construction Materials and Technologies

KÁRMÁN AND THE DEVELOPMENT OF THE MATERIAL MODELS OF CONCRETE

Andor Windisch

DOI: 10.32970/CS.2019.1.1

The failure models developed until the 1960ies were defined by the testing equipment: the triaxial loading cell which was developed at the beginning of the last century by Kármán. The axial loading was performed with a solid loading plate, the central-symmetric transverse loading through hydraulic pressure. Therefore, the characterization of the failure surface with the hydrostatic normal stress and octahedral shear stress without any reference to deformations was a logical consequence.

In 1963 Hilsdorf proposed a brush-type loading equipment. Using brushes Kupfer carried out his well-known biaxial loading tests which made possible the characterization of concrete strength by means of the principal stresses. In 1977 Ottosen applied in his model for multiaxial strength of concrete the stress invariants. The same did CEB in the Bulletin d'Information N°. 156.

Van Mier (1984) applied brushes and proposed a 3D-type representation using contour lines.

The MC2010 returned to the Ottosen model and declared concrete as frictional material.

Using the principal stresses, a new, transparent (and physically really sound) form of representation of the failure surface showing the strength increase due to bi- and triaxial loading is presented.

Keywords: multiaxial strength of concrete, bi- and triaxial loading, triaxial loading equipment, loading with brushes, hydrostatic normal stresses, octahedral shear stresses, principal stresses.

1. RESEARCH SIGNIFICANCE

Kármán's achievements in the aerodynamics are well known but in materials science (e.g. theory of elasticity and plasticity) are less, maybe because these early findings were published in Hungarian and German. Besides developing the triaxial loading equipment in 1910 he pointed out the shortages of Mohr's theory. Although, his triaxial equipment could not produce an independent intermediate principal stress, Kármán emphasized the importance of this stress at the development of concrete strength. The renunciation from the principal stresses to the hydrostatic/octahedral stresses and to the intransparent and material-strange (but elegant) stress invariants governed until MC2010 the characterization of concrete behavior. It is high-time to return in MC2020 to the real material characteristics: concrete „knows" the principal stresses only. This allows a transparent computer/material-friendly description of concrete, high- and ultrahigh strength concrete, too. The paper presents a new type of description of 2D and 3D strength of concrete.

2. KÁRMÁN'S THEORY OF MATERIALS AND HIS TRIAXIAL LOADING EQUIPMENT

Before reporting on the development of his triaxial loading equipment and the results of his related experiments, Kármán (1910) overviews the relevant design hypotheses:

„The question to which I would like to contribute is what is the allowable level of loading? If we know the maximum allowable value of stress or elongation for a material in the case of simple tensile or compressive loading, how can we deduce from this a different kind of stress, e.g. in case of torsion or a complex stress state? The permissible stress for brittle materials is usually based on the fracture, while for plastic and ductile materials it is based on the limit of elasticity, therefore judging the allowable stress requires the knowledge of the limit of elasticity and of the fracture. Since all stress states can be characterized by the values of the three principal stresses, the question is, which function of these three is governing these limits?"

He identified that neither the highest principal stress, nor the deformation work as hypothesis are suitable for determination of the acceptable degree of exploitation.

„In the following, I would like to briefly describe the current hypotheses, highlighting the points that have not yet been decided, which have provided an opportunity for my later experiments:

- the highest principal stress guides the limit of elasticity (Lamé, Clapeyron)
- deformation work is the right measure of degree of loading.

Both hypotheses are contradicted by the simple fact that in a hydrostatic load condition, the material can be subjected to much greater stress and a much larger amount of work can be accumulated in it without reaching the limit of elasticity as one-way compression.

The remaining two hypotheses are

a) largest linear dimension change (which origins from de Saint Venant). Even if at that time different limit values were proposed for the elongation and shortening, the test results contradict this theory.
b) Coulomb's theory (improved by Mohr): the elastic limit depends on the two extreme principal stresses only. The mathematical form of the limit surface is

$$|\tau| = s_0 \pm f\,\sigma \qquad (1)$$

where
τ, σ the shear and normal stresses, resp.
s_0 the constant term of frictional resistance
f friction coefficient."

Kármán asks the question:

„To determine whether the stress state determined by the three principal stresses falls within the elastic limit, it is necessary to examine whether Equ. (1) exists for all directions of displacements? After a simple transformation, we get the expression where it can be seen that the intermediate principal stress is meaningless. Experiments with ductile and plastic materials (iron, copper) largely confirmed the Mohr-Coulomb theory. The mean values of the results of Bauschinger's tensile, compressive and shear experiments with cementitious specimens were to some extent consistent with the demands of Mohr's theory. However, the individual values themselves have such a great scatter, that these experiments hardly can be regarded as demonstrative."

Kármán payed special attention to the tests of Föppl, who examined whether the value of the intermediate principal stress was really irrelevant to the compressive strength. For this purpose, in addition to the ordinary compression test, where only one principal stress is not zero, the materials are subjected to a stress state having equal pressures in two perpendicular directions and zero in the third direction only. Föppl's experiments have shown that the two strengths are nearly equal when a lubricant is applied to reduce the friction between the pressure plates and the specimen, but are very different when the specimen is in direct contact with the pressure plates. Kármán did not regard these results of Föppl as entirely convincing, especially since his experiments in this regard led to the opposite result.

Kármán envisaged to answer the following questions:
a) In which cases does the limit of elasticity depend only on the maximum and minimum principal stresses, in which cases has the intermediate principal stress influence, or in which cases is the difference of the two extreme principal stresses governing?
b) In which cases does a tensile failure and in which cases does a slippage occur, i.e. what conditions should exist between the principal stresses, that one or the other case occur?

The following objectives governed the design of the experimental equipment: the principal stresses could be changed independently, preferably with a homogeneous stress distribution. Instead of combining various loading types (e.g., axial tension, twisting, internal pressure, as other researcher did), experiments with compressive and tensile axial loading were designed with simultaneous application of a uniform transverse fluid pressure. With this arrangement, it was possible to create two rows of states stress: either the two smaller or the two higher principal stresses were equal

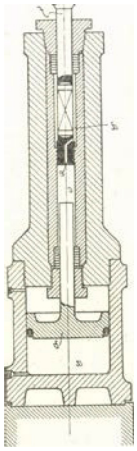

Figure 1: Longitudinal section of the triaxial loading equipment (original drawing in Kármán (1910))

(considering the compression stress positive) the former experiments were called compression tests, the latter tensile tests.

Although, the experiments carried out with the two equal principal stresses are not able to determine the final questions, nevertheless Kármán hoped to receive (at least) guidance on general tests with unequal principal stresses.

The equipment was produced by the steel company Krupp, based on Kármán's designs. *Fig. 1* shows the longitudinal section of the device. The diameter of the hole in the inner tube was 50 mm and the upper limit of the transverse pressure was 6000 atm. Pressure was measured with a manometer, longitudinal deformation indirectly with two micrometer screws. The diameter of the marble and sandstone specimens was 40 mm, their length was between 100 and 110 mm.

During the tests no direct observations of the specimens were possible.

A brief summary of the results of the compression tests: in these cases neither the difference

$$\sigma_1 - \sigma_2, \quad \text{nor} \qquad \sigma_1 - \lambda\,\sigma_2 = \text{const.}$$

characterize the limit of elasticity.

In his second paper dated 1915, Kármán adds the question: which states of stresses cause the failure of the material?

„If we interpret the three principal stresses as spatial coordinates, a certain state of stress corresponds to every point in the space. Thus, in this representation, the elastic limit corresponds to a surface which encompasses the portion of space representing the stress states associated with the purely elastic deformation. This surface is commonly referred to as the limit surface of elasticity. Similarly, a surface is given by the stress states in which the continuity of the material ceases. This second interface can be called the fracture interface.

His conclusions are:
- The elastic limit or the compressive strength varies with the lateral pressure. The elastic limit at low values of the difference of the principal stresses is approximately proportional to the transverse pressure, later this influence decreases, at high lateral pressure it depends only on the difference of the principal stresses.
- The deformation curve of the material depends on the magnitude of the transverse pressure.
- The characteristic angles of the surface drawings are not characteristics of the material, but of the stress state at limit state of elasticity.

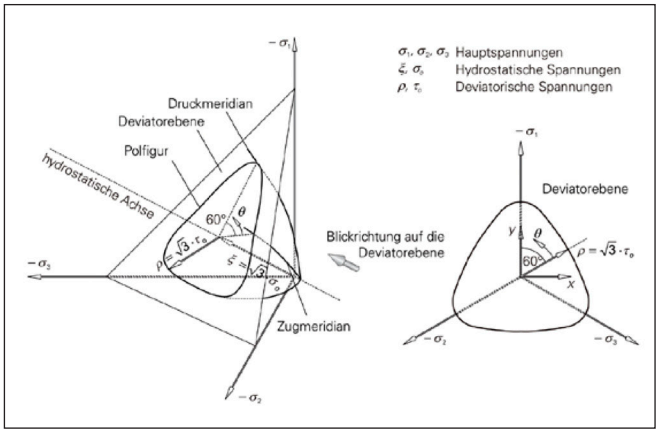

Figure 2: *Designations in 3D stress space (Hauptspannungen: principal stresses; Deviatorebene: deviator plane; Blickrichtung auf die Deviatorebene: outlook to deviator plane)*

- The formation of surface drawings is related to the inhomogeneity of the material and the nature of the deformation curve and can be explained by the distribution of the residual deformation.
- The moment of fracture is not independent of the flexibility of the testing machine and the clamping of the specimen, and the speed of the loading (and unloading).“

It should be noted here, that the influence of the friction between the load piston surface and the specimen are indisputable.

Concerning the further parts of this paper, it should be diagnosed, that in 1910 Kármán already knew that the Mohr-Coulomb-theory does not fit for concrete-like materials and the stress state must be characterized through the three principal stresses.

3. HISTORICAL REVIEW

The failure models developed until the ‘60ies of the last century were defined by the testing equipment: the triaxial loading cell, developed by Kármán. As the transverse stresses (two of the three principal stresses) were equal, hence the threefold discrete rotational symmetrical characterization of the failure surface with the hydrostatic normal stress and octahedral shear stress was a logical (but extremely intransparent) consequence. *Fig. 2* shows the basic notions and designations of this type of characterization. The description of the results of the tests with a Kármán-type equipment with the compressive and tensile meridians was also obvious:

Compressive meridian: $\sigma_1 = \sigma_2 > \sigma_3$ with $\sigma_1 \geq \sigma_2 \geq \sigma_3$
Tensile meridian: $\sigma_1 > \sigma_2 = \sigma_3$ with $\sigma_1 \geq \sigma_2 \geq \sigma_3$

Fig. 3 shows the relative positions of the measured values and the mean values vs. a 3D failure criterion: these do not fit at all. *Fig. 3* reveals how intransparent this type of representation is! Try to determine the 2D- or 3D strength for given $\sigma_{1u} / \sigma_{3u}$ and $\sigma_{2u} / \sigma_{3u}$ ratios!

4. CEB BULLETIN NO. 156

In the CEB Bulletin No. 156 the description of “the Ultimate Strength Surface (USS) is based on the following technical considerations and rational reasoning:

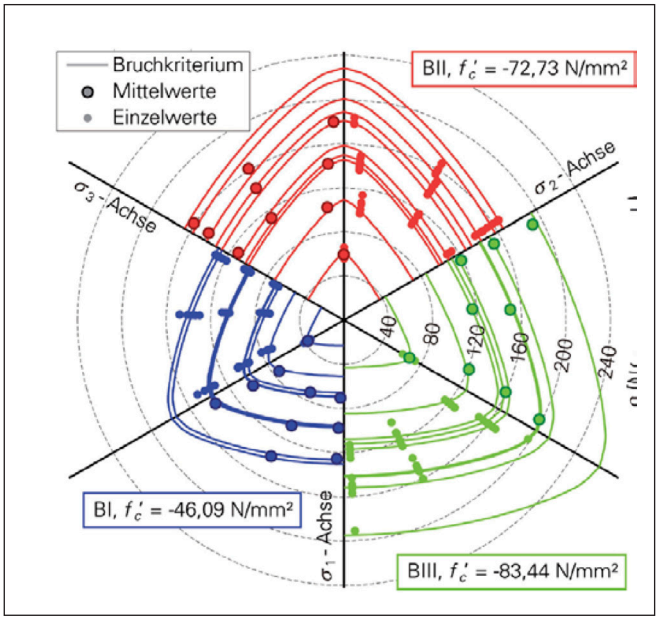

Figure 3: *Relative positions of the measured and the mean values vs. a 3D octahedral failure criterion for three concretes as measured by Speck*

a. USS is to be described by invariants of the stress tensors or by expressions derived from it
b. For an isotropic material without any history, the USS in the deviatoric plane (polar figure) is three-fold symmetric with respect to the hydrostatic axis.
c. Theory of plasticity and more recent fracture mechanics studies require the polar figures to be convex.
d. For a material whose uniaxial compressive strength differs from its tensile strength, one must distinguish between a triaxial compression curve and a triaxial tension curve.”

Comments of the author:

To a): as well known, the invariants of a tensor (here the stress tensor) do not change with the rotation of the coordinate system. The proposed description of USS by invariants makes the stress state non-transparent and less practical. Much better is to transfer any stress state into its principal stresses with the corresponding directions. The material concrete “perceives” principal stresses only. The description by hydrostatic normal stress and octagonal shear stress was essential as at the early experiments in the triaxial cells only one principal stress was explicit; all transverse directions were “principal” directions. The hydrostatic and octagonal stress components “helped” to overcome this “difficulty”.

To b): due to its production technology (pouring) concrete is not isotropic. In the era of the high capacity computers there is no reason to adhere to the not existing material isotropy.

To c): recent test series (van Mier (1983), Speck (2007)) revealed that -especially in case of concretes beyond C40- theory of plasticity cannot be applied to concrete. The “plasticity” of RC slabs results from the “residual elasticity” of the concrete compression zone of slightly reinforced cross sections: reference shall be made to the limit of mechanical rate of reinforcement at plastic moment redistribution of slab systems, see EC2 (1997) and MC2010 (2012). It is not the concrete material itself, but this plasticity attributed to the concrete compression zone ”results” from the difference between the depth of compression zone calculated assuming perfect bond between rebars and concrete and the real behavior of the cracked RC section, provided that low amount, moderate diameter rebars are applied. Incidentally

the USS described as function of the principal stresses is always per se convex.

To d): the triaxial compression curve (or meridian) and the triaxial tension curves are direct "results" of the physical possibilities of the triaxial cells: the stresses in the transversal directions were always identical, which corresponds to the definition of these meridians. In a description of the USS in the coordinate system of principal stresses these meridians are meaningless.

"The experimental studies have shown that ultimate strength of concrete subjected to multiaxial stresses is controlled by the propagation of microcracks. These microcracks are mainly orientated in one (or both) perpendicular direction to the direction of the smallest principal compressive stress (or the two, if their magnitudes are similar) of the largest principal tensile stress."

In the following CEB Bulletin N°156 proposed to apply Ottosen's theory, see later in Chapter 6.

5. *VAN MIER*

The most important basic statement of van Mier (1984) is: All experiments, also the uniaxial ones, are/must be essentially considered as triaxial.

The strength envelopes for bi- and triaxial experiments by van Mier (see *Fig. 4*) are very transparent and informative. One comment: the validity of the level lines could be questioned: the reciprocity of the strength values $f_u(0;0.1;1)$ and $f_u(0.1;0;1)$ 47 vs. 56 N/mm² is not given. This could be originated from the different concrete batches of the series of relevant specimens. Accordingly, no reliable extrapolations for higher confining stress levels are possible.

Making use of the sense of the strength envelops for bi- and triaxial experiments published by van Mier (see *Fig. 4*)

Figure 4: *Van Mier's (1984) strength-envelopes for the bi- and triaxial experiments. (The tensile axis σ_2 is drawn in a larger scale!)*

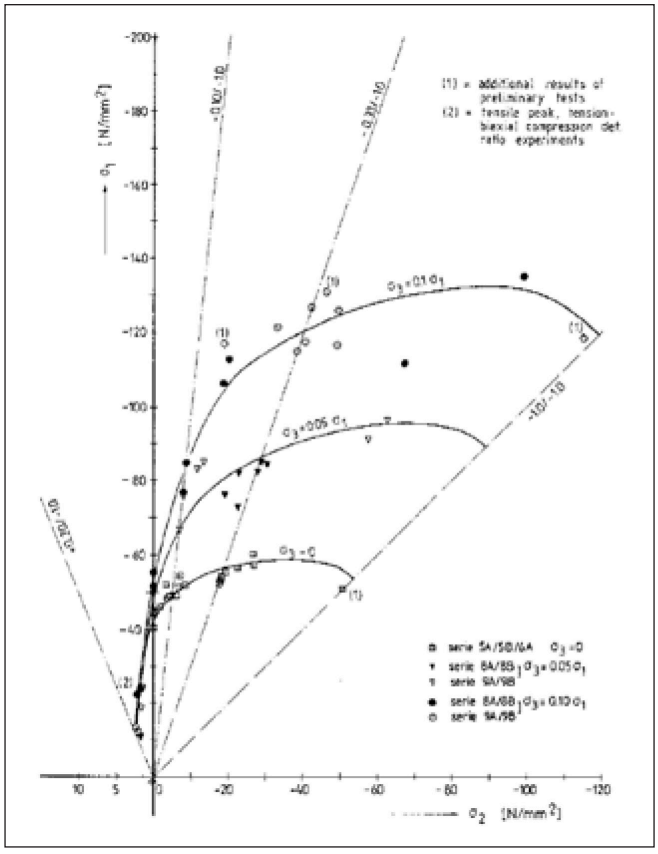

the following dimensioning and control tasks can be followed (the envelopes of the concrete class regarded are known):

- Dimensioning: in case of a given concrete class the strength $f_c^* > f_c'$ shall be reached. $f_c^* > f_c'$ can be achieved along the line $\sigma_3 = f_c^*$ parallel to the σ_2-axis. It must be checked what kind of constrictions perpendicular to the direction of f_c^* (i.e. γ and λ) are given/possible. γ means the steepness of a line in the σ_2-σ_3 plane through the origo; λ is the coordinate of the elevation contour line of the failure surface parallel to the σ_2-σ_3 plane. The intersection of the $\sigma_3 = f_c^*$–line with the line with the steepness of γ in relation to the next two λ-contours along the γ-line gives the necessary rate of confinement in the direction of σ_1.
- Control: concrete class, γ and λ are given. The position of the point along the γ-line corresponding to the λ-ratio shall be determined. The σ_3 ordinate of the intersection is the achievable strength, f_c^*. If the $\sigma_3 \geq f_c^*$ then the strength criterion is fulfilled, otherwise
  - either the rate/s of confinement shall be changed or
  - a higher concrete class shall be chosen.

  As in the tests
- the most possible endeavor was made to have the principal axis parallel with the sides of the cubic specimens,
- the principal components are the most fundamental characteristics of any state of stress
- concrete (and the specimens, too) are never isotropic (at least the direction of compaction have some significant impacts)

hence any transition to the invariants of the deviatoric stress tensor is rather meaningless.

Some discusser called in question the raison d'être of applicability of the loading path and try to consider the problems as uniaxial ones (see the nonlinearity index and the stress-strain behavior splitted in three independent uniaxial characteristics of Ottosen). Van Mier and its *Fig. 4* teach us: any target 3D ultimate strength can be reached following a loading path only: with a 2D loading an increase of 10-20% maximum can be achieved only. Beyond this level loading/strain restriction in the third direction are necessary to let increase the maximum compressive strength in the 'main/leading' direction.

6. *MC2010*

Dealing with the multiaxial states of stress in concrete, MC2010 (2013) treats concrete as frictional material. "The multiaxial criteria should depend not only on shear stresses, but also on the first invariant I_1 of the stress tensor to consider the influence of the hydrostatic pressure on the ductility of the material."

As it could be known since Kármán, concrete is not a "frictional material". Moreover, it has neither a yield function but a failure criterion, nor a flow rule/plastic potential. Especially in case of higher-class concretes after the principal stresses fulfil the failure criteria the concrete loses dramatically its load-bearing capacity, hence its behavior does not allow for a treatment as a "plastic material". Any transformation of the non-linear stress-strain curve into a linear-elastic-"plastic" working diagram (even if with retaining the area under them) falsifies the real character of concrete.

Among several acceptable formulations MC2010 has chosen the constitutive equation of Ottosen as "it is not too difficult to use and agrees well with test data".

The mean value of strength under multiaxial states of stress may be estimated from the failure criterion

$$\alpha \frac{J_2}{f_{cm}^2} + \lambda \frac{\sqrt{J_2}}{f_{cm}} + \beta \frac{I_1}{f_{cm}} - 1 = 0$$

where

$$\lambda = c_1 \cdot \cos\left[\frac{1}{3} \cdot arccos(c_2 \cdot cos3\theta)\right]$$

$$\cos 3\theta = \frac{3\sqrt{3}}{2} \cdot \frac{J_3}{J_2^{3/2}}$$

I_1 is the first invariant of the stress tensor, J_2 and J_3 are the second and third invariants of the stress deviators. In mathematics, an invariant is a property, held by a class of mathematical objects, which remains unchanged when transformations of a certain type are applied to the objects.

(Note: Zhou (1995) recalled that according to the basics of tensor analysis I_1 and $\sqrt{J_2}$ are linearly dependent of each other; hence the formula of Ottosen could be simplified.)

The coefficients α, β, c_1 and c_2 are material parameters which depend of the uniaxial compressive strength f_{cm}, the uniaxial tensile strength f_{ctm}, the biaxial compressive strength f_{c2cm} and the triaxial compressive strength at one point of the compressive meridian ($\sigma_1 = \sigma_2 > \sigma_3$) described by σ_{com} and τ_{com} (these two are the octahedron stresses). In order to determine these coefficients five additional parameters have to be calculated. (Note that f_c and f_{c2c} are defined as positive values; all other compressive strengths are negative values.)

It must be diagnosed that the Ottosen model is extremely intransparent.

7. NEW 3D REPRESENTATION OF MULTIAXIAL STRENGTH OF CONCRETE

The most important basic statement: All experiments, also the uniaxial ones, are/must be essentially considered as tri-axial. All possible combinations of stresses which correspond to an ultimate stress state can be expressed in terms of relative principal stresses as an ultimate strength surface (USS).

The stress state in a point is characterized with the three principal strength values. These are ordered as follows: $\sigma_1 \geq \sigma_2 \geq \sigma_3$. Compressive stresses and strains are negative, the tensile ones are positive.

The following notations are introduced:

- Stress state is described in vector form in terms of the principal stress components,
- The loading occurs along a "loading path", i.e. during loading the ratios $\gamma = \sigma_1 / \sigma_3$ and $\lambda = \sigma_2 / \sigma_3$ remain constant, the triade (γ; λ; 1) characterizes a stress-loading path,
- $f_{cu}^* = \sigma_{3u}$ is most negative strength at failure along any stress-loading path.

Accordingly, $\sigma_{1u} = \gamma\, \sigma_{3u}$ and $\sigma_{2u} = \lambda\, \sigma_{3u}$.

The invariants of the stress and (especially) of the strain tensors remain –as non-transparent and misleading quantities - ignored. Accordingly, the hydrostatic axis, the deviatoric plane, the requirement for the (not realistic) three-fold symmetry and the convexity of the polar figures disappear, too. Similarly, the triaxial compression curve and triaxial tension curve (meridians) in the Rendulic plane vanish.

The hydrostatic stress and strain and the octahedral shear stress and strain hinder the examination of the impact of the three (maximum, intermediate and minimum) principal stresses and strains on the failure surface.

Notions as "equibiaxial" and "equitriaxial" tensile strengths disappear as well: in an equibiaxial tensile test the tensile failure will occur according to the scatter of the tensile strength, independent of each other in the two directions. The same is valid for the equitriaxial tensile tests. The reason is, that –in contrary to the compressive loading, where in transverse direction to the compressive stresses micro- and later macro-cracks occur which influence the actual strength there- the tensile failure occurs in a 'thin' region only perpendicular to the direction of tensile force hence does not influence the tensile strength in the two other directions (See Fictitious Crack Model of Hillerborg et al. (1976)).

The results of the 2D and 3D tests (σ_{3u}) will be displayed in the coordinate system γ, λ as $\sigma_{3u} = f(\gamma, \lambda)$.

Advantages of this display are:

- The direct impact of the maximum and medium stresses, resp. can be perceived.
- As $\gamma \leq 1$, $\lambda \leq 1$ hence the USS has "natural limits" at $\gamma = 1$, $\lambda = 1$.

It should be recognized that for each concrete class only two failure configurations characterized with the triade (γ; λ; 1) exist:

- the direction of σ_{3u} coincides with the direction of the pouring/compaction,
- it does not coincide.

This means that each failure surface displayed in the (σ_1, σ_2, σ_3) coordinate system is monovalent over the (σ_1, σ_2)-plane. The description using the octahedral stress components suggests an axis-invariance which in the case of concrete (if only because of the direction set by the compaction) might lead to faulty assumptions as due to its production technology concrete is not isotropic. This is even truer in case of fiber reinforced concrete. *Fig. 5* shows the proposed 3D representations of van Mier's results presented in his Fig. 5.8 (1984) and Speck's results with a C80/95 concrete.

One advantage of this type of representation is that in the $\gamma = \sigma_1 / \sigma_3$ direction no special function with regard of a strength under hydrostatic loading conditions must be found. The renunciation of the hydrostatic- and deviator-related representation yields a

- clear and transparent understanding of the influence of the minor (γ)- and intermediate- (λ) stress levels resp.,
- deviating from the compulsory three-fold symmetry with respect to the hydrostatic axis the figures meet the non-isotropic characteristics of the concrete which is the direct consequence of concrete production technology (pouring). It is even more pronounced in case of the fiber-reinforced concretes, which are more and more coming.
- It reveals how misleading is the validation of the Ottosen model using the uniaxial compressive strength (point on the compressive meridian), biaxial compressive strength (point on the tensile meridian), a triaxial compressive strength at one point on the compressive meridian (plus the uniaxial tensile strength). Note: With her very advanced test equipment Speck achieved $\gamma = \lambda = 0.15$ only. Anyway: the strength values along the compressive meridian are of very limited informative value. The maximum strength increase could be anticipated with $\gamma = \lambda = 0.5 \sim 0.6$. The double-curved surface of the failure surface does not allow any reliable extrapolation relying on $\gamma = \lambda = 0$ and $\gamma = \lambda = 0.15$.

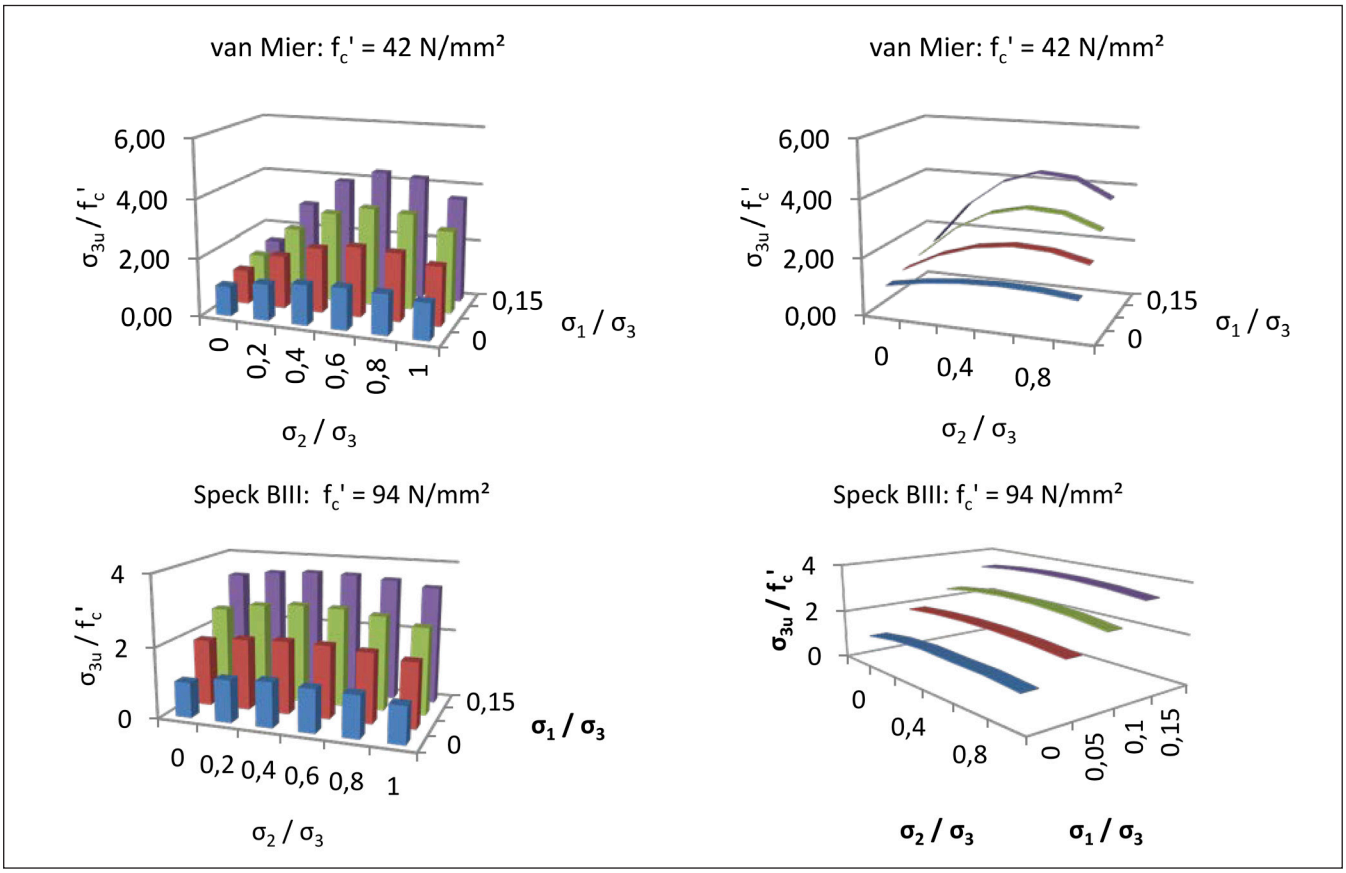

Figure 5: New type representation of the strength increase of two classes of concrete (van Mier and Speck)

8. CONCLUSIONS

Kármán's – relatively unknown – theoretical considerations from 1910, related to elasticity and plasticity of ductile and brittle materials and his triaxial loading equipment are presented. The possibilities and restrictions of this equipment determined for 100 years the theoretical and practical works with concrete strength. After a review of some works a new-type 3D representation of triaxial concrete strength is proposed which is transparent and physically sound.

9. NOTATIONS

I_1	first invariant of the stress tensor;
J_2, J_3	second and third invariants of the stress deviators
f_c'	concrete compressive strength
f_{cu}*, f_{ct}*	ultimate strength (compression and tension resp.) in 2D and/or 3D loading
α, β, c_1 and c_2	material parameters (Ottosen)
$\gamma = \sigma_1 / \sigma_3$	loading parameter
$\lambda = \sigma_2 / \sigma_3$	loading parameter
σ_1, σ_2, σ_3	principal stresses ($\sigma_1 \geq \sigma_2 \geq \sigma_3$)
σ_{c3u}	ultimate strength measured in test
σ_{com}	hydrostatic normal stress
τ_{com}	octahedral shear stress
[γ; λ; 1]	stress-loading path
$[1;1;\sigma_{c3u}]$	ultimate hydrostatic normal strength (cap value)

10. REFERENCES

Bauschinger, (1879): „*Mittheilungen aus dem technisch-mechanischem Laboratorium*", München, Heft 8.

Comité Euro-international du Béton, Bulletin d'information N° 156 (1983): "Concrete under multiaxial states of stress. Constitutive equations for practical design", Contribution à la 23e Session plenière du C.E.B. Prague – Octobre 1983, Juin 1983, pp. 149.

Föppl, (1900), *Phil. Mittheilungen aus dem technisch-mechanischem Laboratorium*, München, 27.

Kármán, von, Th., (1909): „ Untersuchungen über Knickfestigkeit", Berlin, 37 p. *Mitteilungen über Forschungsarbeiten auf dem Gebiete des Ingenieurswesen*.

Kármán, von, Th., (1910): „Mitöl függ az anyag igénybevétele? (in Hungarian: What determines the stress-strain behavior of matter?) *Journal of the Society of Hungarian Engineers and Architects*, Vol. XLIV, X., pp. 212–226.

Kármán von, Th. (1915): "Vizsgálatok a rugalmassági határ és a törés feltételeiröl", *Mathematikai és Természettudományi* Értesítő, Magyar Tudományos Akadémia, XXXIII, pp.1-50. Budapest, 1915 (Lecture held at the meeting of MTA Div. III on 17th October 1910.

Hillerborg, A., Modéer, M., Peterson, P.E. (1976): "Analysis of crack formation and crack growth in concrete by means of fracture mechanics and finite elements", *Cement and Concrete Research*, Vol. 6, 1976, pp. 773-782. https://doi.org/10.1016/0008-8846(76)90007-7

Hilsdorf, H. (1965): „Versuchstechnische Probleme beim Studium der zweiachsigen Festigkeit des Betons", Sonderdruck Heft 173 der *Schriftenreihe des Deutschen Ausschusses für Stahlbeton*, 1965.

Kupfer, H., (1973): „Das Verhalten des Betons unter mehrachsiger Kurzzeitbelastung unter besonderer Berücksichtigung der zweiachsigen Beanspruchung", *Deutscher Ausschuss für Stahlbeton*, Heft 229, Ernst und Sohn, Berlin, p. 105.

Mier, van, J.G.M., (1984): „Strain-Softening of Concrete under Multiaxial Loading Conditions", Dissertation, TH Eindhoven, p. 363.

Ottosen, N.S., (1977): „A Failure Criterion for Concrete", *Journal of Engineering Mechanics*, Div. ASCE, Vol 103, EM4, Aug. 1977

Ottosen, N.S., (1981): "Constitutive Models of Concrete Versus Recent Experimental Data", *Risø-I-72*, Risø National Laboratory, Roskilde, Denmark, June 1981

Zhou, Y. (1995), "Über das Festigkeitsverhalten verschiedener Werkstoffe", *Bericht aus dem Bauwesen*, Aachen, Shaker Verlag.

Andor Windisch PhD, Prof. h.c. retired as Technical Director of Dywidag-Systems International in Munich, Germany. He made his MSc and PhD at Technical University of Budapest, Hungary, where he served 18 years and is now Honorary Professor. Since 1970 he is member of different commissions of FIP, CEB and ***fib***. He is author of more than 180 technical papers. Andor. Windisch@web.de

PRELIMINARY ANALYSIS OF AN RC CONTAINMENT STRUCTURE SUBJECTED TO AIRCRAFT-IMPACT


Lili Eszter Hlavicka-Laczák – György Farkas

DOI: 10.32970/CS.2019.1.2

Analysis of aircraft impact is required for newly designed nuclear power plant containments, that are typically robust reinforced concrete (RC) or prestressed concrete structures. In our paper we shortly summarize the main function of containments and show some typical examples for their structural arrangement. From the point of view of the impact we show the typical effects of an aircraft impact and the analysis methods of it. In the second part of the paper a preliminary analysis for aircraft impact into a prestressed concrete containment building is executed with different methods and with a military jet and a large passenger aircraft. At the end results of the analysis are evaluated and suggestions for more detailed modelling are made.

Keywords: nuclear power plant containment, prestressed concrete, aircraft impact

1. INTRODUCTION

The probability of an aircraft impact into conventional engineering structures is extremely low, therefore it is not included in the design standard. However, in case of nuclear power plants (NPPs) or other nuclear related facilities, because of the severe consequences (e.g. release of radioactive substances), aircraft impacts have to be analysed. Beside the safety of operating NPPs it is also important regarding the design of new ones. According to the Hungarian regulations (Government Decree 118/2011) impact of smaller military jets and also of larger civil aircrafts has to be analysed.

In this paper we shortly summarize the functions and arrangement of NPP containment buildings and the effects of an aircraft impact into them. We also present the possible modelling techniques of reinforced concrete and prestressed concrete structures subjected to impact loading.

In the second part of the paper a preliminary analysis is presented where both impact of a military jet and of a larger commercial aircraft is examined into a prestressed concrete containment building. After the analysis the results are evaluated, and suggestions are made for further researches.

2. CONTAINMENT STUCTURES OF NUCLEAR POWER PLANTS

2.1 Functions and arrangement of containment structures

The containment (hermetic protective building) is the structure that surrounds the reactor and the systems directly connected to it. From the structural point of view, it is a pressure vessel that should retain the overpressure that occurs in case of accidents. It also means the final physical barrier between equipment of the nuclear technology and the environment. This barrier function includes the protection of

Fig 1: Schematic cross-section of AP 1000 (Sahlin et al., 2015), EPR (Areva, 2007), VVER-1200 (Aszódi, 2017)

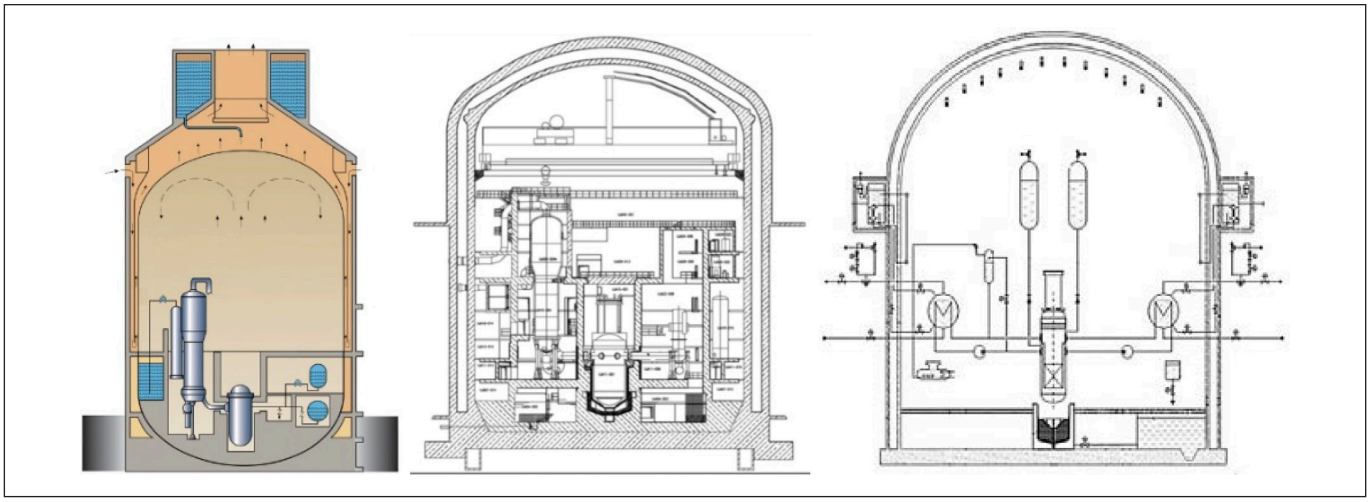

the environment from fission products and ionising radiation and the protection of the internal technology from external natural hazards and human activities (meteorological loads, explosion, fire, aircraft-impact etc.) as well.

Based on the Nuclear Safety Code Vol. 3a 4.6. (Annex 3/A to Government Decree No. 118/2011 (VII.11.)) the containment function can be provided by either one or two separate containment structures. In the latter case, subatmospheric pressure in the space between the two structures should be kept, in order to detect leakage through the inner wall and to prevent the release of radioactive substances into the environment. In case of double-walled containments the protective function is separated: the inner (primary) containment has to be designed for overpressure (that occurs in case of a LB LOCA=large break, loss of coolant accident), while the outer (secondary) for aircraft impact. The inner containment can be a steel vessel with a concrete external shield building (e.g. AP1000, where the inner steel wall is 4.5 cm thick, the outer concrete wall is ~0.9 m with 2 cm thick steel plating (Sahlin et al, 2015)). Instead of a steel inner wall it is also typical to use prestressed concrete, two examples for this are the EPR (European Pressurized Reactor, inner containment: 1.3 m thick post-tensioned concrete with 6 mm metallic liner, outer shield building: 1.3-1.8 m thick reinforced concrete (Areva, 2007)) and the VVER-1200 (inner wall 1.2 m post-tensioned concrete; outer wall: 0.5 m thick reinforced concrete (Asmolov et al., 2017)), see *Fig. 1*.

In case of single-wall containments both protective functions are provided by the same wall, this solution is typical for the NPPs operating since the 70's-90's (Generation II), that were not designed for aircraft-impact. One example is the Unit 3 of Ohi NPP in Japan (see *Fig. 2*), where 1.1-1.3 m thick post-tensioned concrete wall is applied. Another example is the Paks 1 NPP (*Fig. 3*), where VVER-400 reactors operate, in this case a bubble condenser containment building is built, which means a hermetic compartment system in which the steam-air mixture generated within a LB LOCA is transferred into the bubble condenser system where it is condensed and the pressure is reduced (Blinkov et al., 2012).

Fig 2: Ohi NPP, Unit 3 from outside (source: wikipedia.org- Ohi Nuclear Power Plant) and schematic cross-section of the containment (Sandia National Laboratories, 2003)

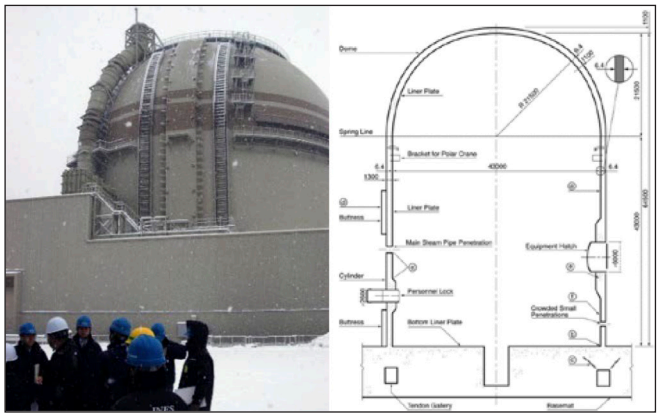

Fig 3: Cross-section of the hermetic compartment system of Paks 1 (without the reactor hall building), (Boros, 2017)

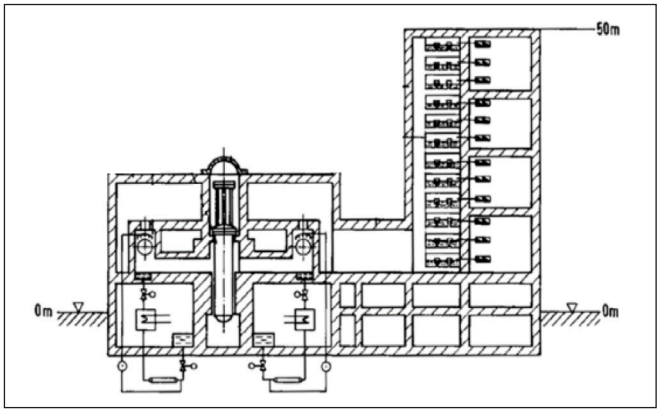

2.2 Design requirements for aircraft impact

Based on the Annex 3/A to Government Decree No. 118/2011 for new NPPs crash of a military or civilian aircraft is included in the design basis, which means that the criteria of design basis (TA) operating conditions have to be met in case of aircraft crash that has higher probability than 10^{-7}/year (that is the frequency limit for external hazard factors associated with human activities). Selection of the aircraft types that have to be analysed is done by taking into account the statistics of accidents and the location of airports near the site of the NPP.

Crash of a military or civilian aircraft is also included in the extension of the design basis: requirements for TAK1 (complex accident) operating condition should be fulfilled. For any possible military or civil aircraft it has to be proved that: a) the cooling of the active core of the nuclear reactor is not compromised or b) the containment is not damaged, and c) the cooling or integrity of the spent fuel pool is maintained. In this case large passenger planes are the critical missiles that have to be examined without analysing the probability of their impact.

3. EFFECTS OF AIRCRAFT IMPACT AND THEIR ANALYSIS

The effects of an aircraft impact into a relatively rigid structure depend on multiple factors. The most important parameters are the size, mass, stiffness of the aircraft, direction and location of the impact and properties of the target structure (containment). The effect of different parameters was analysed in details by Laczák (2017). We can distinguish between two primary effects: global and local effects. The first means the overall structural response of the target structure, while the second means the effects that locally cause significant damages at the impact zone (*Fig. 4*). Beside primary effects, secondary effects such as vibrations, fire, explosion, high temperatures can also be significant. In this paper we mainly focus on global primary effects.

Fig 4: Local effects: (a) penetration, (b) cone cracking, (c) spalling, (d) cracks, (e) scabbing, (f) perforation and global effect (g) of missile impact (Li et al., 2005)

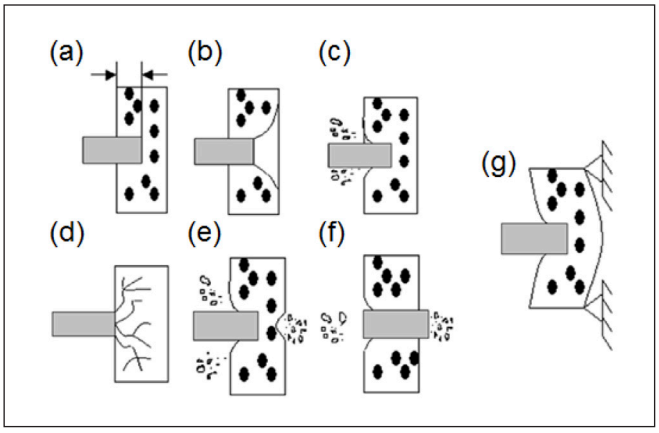

Fig.5: Full-scale impact test of a Phantom F4 fighter (Sugano et al., 1993-1)

The damage caused by the aircraft or its parts to a great extent depends on the stiffness and rigidity of the missile and the target. Usually, an aircraft fuselage that impacts a concrete structure with thick walls means a deformable (soft) missile causing global effects while the engine behaves as a non-deformable (hard) missile that causes local effects (penetration, perforation, scabbing). A detailed full-scale test series was done by Sugano et al. using a Phantom F4 fighter (*Fig. 5*) and its engine (Sugano et al., 1993-1,2,3). In general, different models and methods are used for the analysis of global or local effects, we will discuss them shortly in the following.

3.1 Global effects

Global effects are mainly caused by deformable missiles, such as the fuselage of an aircraft if the impact velocity is sufficiently high and the target is sufficiently rigid. In this case the impact can be substituted by a load-time function acting on the target. Such load-time functions are prescribed by the standards (Katona, 2015) or can be determined by different analytic methods, from which the most frequently used is the Riera method (Riera, 1968). Both the method of Riera and the lumped-mass model of Wolf (1978) have been verified during the experiment of Sugano et al. (1993-1), as the calculated load-time function approximated well the measured impact force-time function acting on a rigid wall during the test shown in *Fig. 5*. The calculated and measured load-time functions are presented in *Fig. 6*.

Fig 6: Load-time function in case of impact of a Phantom F4 fighter with 215 m/s, (based on Riera (1968), Wolf (1978) and Sugano et al. (1993-1))

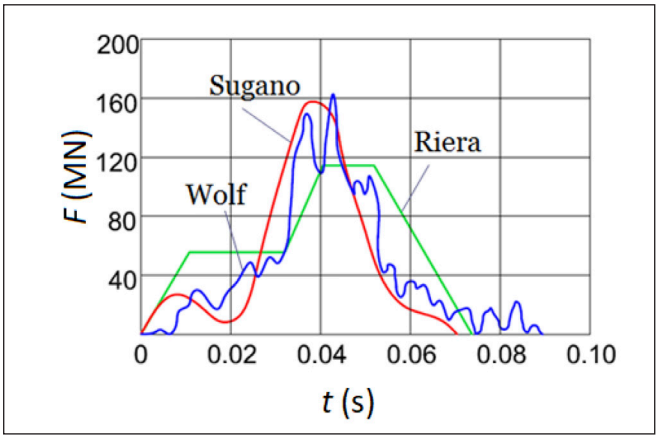

As the available computational capacity increases, application of detailed numerical models that includes both the aircraft and the containment becomes possible, this analysis type is called missile-target interaction method. On the one hand these models can provide detailed information on the behaviour of the structure and of the missile. On the other hand, several parameters appear in these advanced models, which can lead to uncertainties, therefore the application of load-time functions for calibration of detailed models is still relevant. For preliminary analysis it is also suggested to use a linear elastic target by assuming that the effects of nonlinearity are only important in the vicinity of the impact zone. Two examples for detailed numerical models for the analysis of global effects are shown in *Fig. 7*. Both use volume elements with concrete material model and the reinforcement is modelled by constrained line elements.

3.2. Local effects

The local effects are typically dominant when the deformations of the missile are negligible compared to the damages of the target. Local damages are material specific, the most important effects in case of RC structures are shown in *Fig. 4*. From the point of view of the barrier function of the containment building the most important parameters are the required thicknesses to prevent perforation or scabbing. In case of scabbing the missile does not perforate the target, but the formation of debris (secondary missiles) can also cause damage in the protected zone. The determination of the required thicknesses is done by analytic, semi-empirical and numerical calculation methods. Summarizing articles on local failure calculations were published by Kennedy (1976), Teland (1998), Li et al. (2005) and Murthy et al. (2010). An example for numerical tests is shown in *Fig. 8* where a quarter model of a wall is shown for a rigid bullet impact. The applied material model is an advanced explicit material model for concrete, that can follow the local damages (compaction, penetration, scabbing). Red colour represents the totally damaged elements, while blue colour shows the intact parts.

Fig 7 left: Model of the impact of a Boeing 747 into a fictious containment building (Arros, 2007); right: model of an RC containment and the damage after impact of a Phantom F4 (Iqbal et al., 2012)

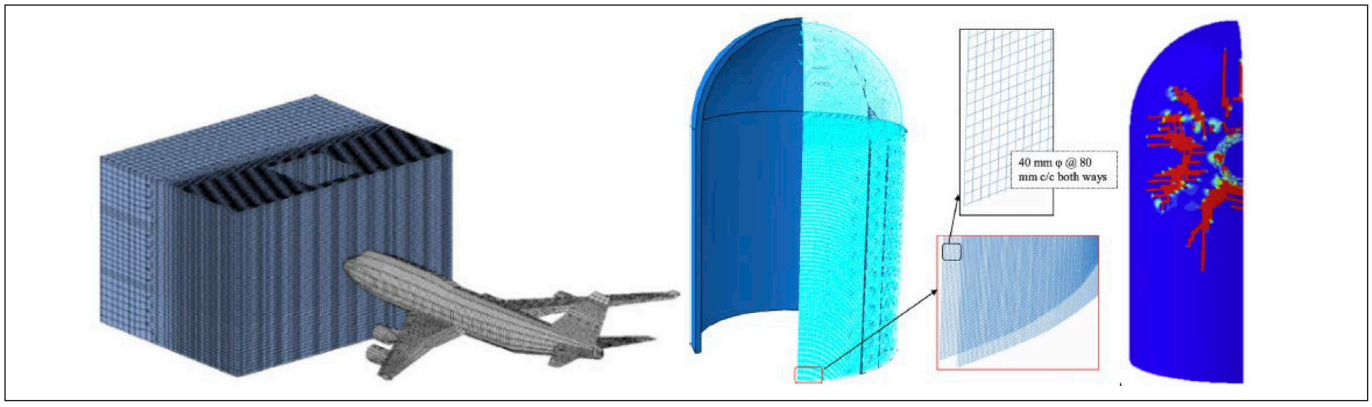

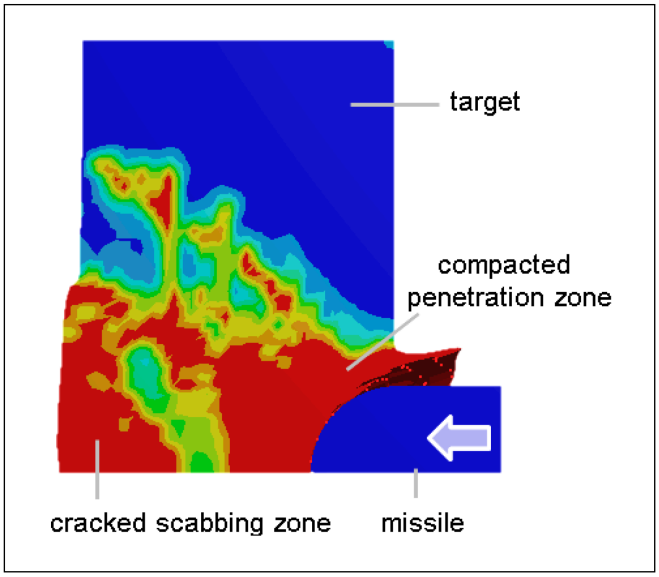

Fig 8: Damage of a concrete target in case of impact of a rigid missile, red colour represents the totally damaged elements, blue colour shows the intact parts (Laczák and Károlyi, 2016)

4. PRELIMINARY ANALYSIS OF A CONTAINMENT STRUCTURE

As a case study, preliminary analysis of a containment with simplified geometry and prestressing of the Unit 3 of the Ohi NPP is done for the impact of a Phantom F4 and of a Boeing 747 aircraft, the impact velocity is 215 m/s in both cases. The containment building was chosen because it was examined in details during a 1:4 scale overpressurization test (Sandia National Laboratories, 2003), therefore details of its pre-stressing system are available. The mentioned aircraft types were chosen because they are frequently used in the related literature.

4.1 Numerical model

The finite element (FE) model is built in Ansys Workbench Explicit Dynamics environment. The model of the containment building consists of a cylindrical building with hemispherical dome. Linear elastic volume elements are used (Young's modulus 35 GPa, Poisson ratio 0.2, density 2500 kg/m^3), the reinforcement is not modelled. The wall thickness is 1.2 m, the height of the cylinder is 43.0 m, total height of the structure is 65.7 m, outer radius of the cylinder and of the hemisphere is 22.7 m, average element size is ~1m (*Fig. 9*). We do not take into account that Young's modulus of concrete depends on the loading rate. The design overpressure of the Unit 3, Ohi NPP containment is 0.47 MPa, therefore its prestressing system was designed to provide decompression in case of such overpressure. In the model, effect of prestressing is taken into account by -0.47 MPa negative internal pressure, that points towards the interior and acts in the normal direction of the internal surface of the cylinder and of the hemisphere. The calculation is done in two steps: at first, static analysis is done with application of the prestressing, then in the second step the results of the static calculation are used as initial conditions for the explicit dynamic analysis. In case of the Phantom F4 both a load-time function and a missile-target interaction model are used, while for the Boeing 747, only a load-time function is applied. Normal directional impact at the connection of the cylinder and the hemisphere are investigated (see *Fig. 9* left). In case of the load-time function the load is distributed on a circular surface with 3 m diameter.

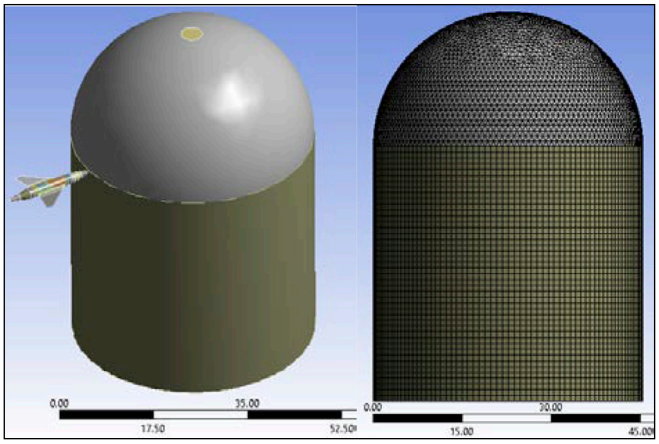

Fig 9: Geometry of the containment and the Phantom F4, and FE mesh of the containment

4.2 Analysis of military jet impact

Impact of a Phantom F4 fighter is examined at first. The load-time function is a simplified function determined by the Riera method. For the missile-target interaction model a simplified aircraft geometry is used with bilinear kinematic hardening material (initial Young's modulus 200 GPa, hardening modulus 2 GPa, Poisson ratio 0.3, limit stress 30 MPa, density 5500 kg/m^3), the finite elements of the aircraft fail and are deleted from the model if limit compressive strain value 1.0 is reached. Length of the aircraft is 17.5 m, its mass is 4655 kg+2626 kg+12208 kg=19.5 tonnes (wings + engines + fuselage). Wall thickness in the model is 2.5 cm for the fuselage and wings, 10 cm for the engines, average FE size is 0.2-0.4 m.

Fig. 10 shows the load that acts on the containment wall, which is the load-time function in one case and the measured contact force-time function in case of the missile-target interaction. Difference between the two can be explained by the difference in the engines' stiffness in the FE model and in the model with load-time function. By more detailed modelling of the engines the difference can be reduced. Crushing of the model aircraft is shown in *Fig. 11*.

Fig. 12 shows the horizontal displacement of the containment as a function of time at the middle point of the impact zone. The shape of the displacement-time functions follows the shape of the force-time functions, maximum displacements from the linear elastic model are 0.028 m (missile-target interaction method) and 0.036 m (load-time function). Global structural behaviour of the containment in case of the load-time function can be followed in *Fig. 13*, where horizontal displacement of the top of the dome (at

Fig 10: Load that acts on the containment in case of missile-target interaction method and in case of application of the load-time function

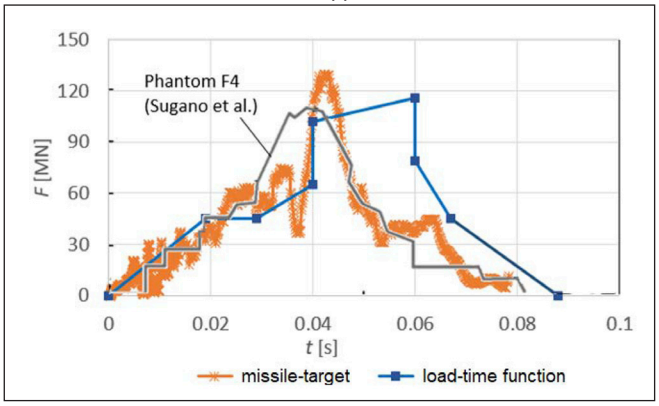

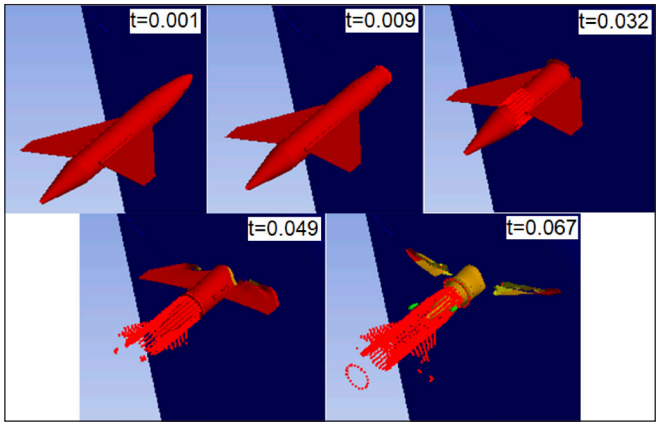

Fig 11: Crushing of the model aircraft (time is given in seconds)

height h=65 m), horizontal displacement at the middle of the impact zone (at height h=43 m (max)) and at the height of the impact but at the point farthest from the impact (on the other side of the building, at height h=43 m (min)) are shown. It is visible that the cantilever-like horizontal deformation of the building is small (the top of the containment moves only 0.01 m) compared to the local displacement in the impact zone. The maximum (linear elastic) tensile stress also arises at the impact zone, it is 26.2 MPa in case of the missile-target method and 37.7 MPa in case of the load-time function, the magnitude of the tensile stress shows that crack formation and nonlinear behaviour should be considered in the impact zone. This magnitude of stress shows that detailed analysis is needed with nonlinear and concrete specific material models as such tensile stresses cannot occur in concrete.

Fig 12: Horizontal displacement of the containment at the impact zone in case of missile-target method and in case of application of the load-time function

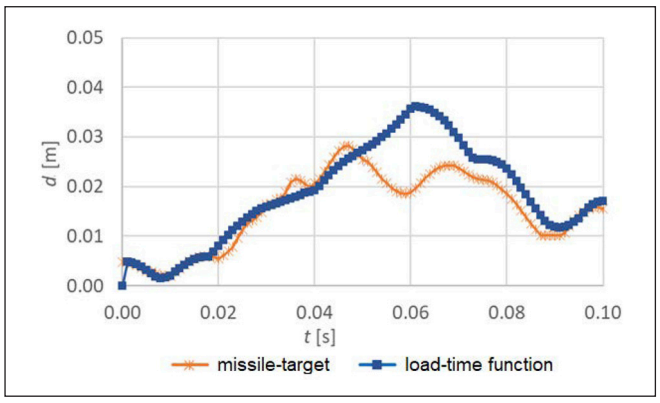

Fig 13: Maximum horizontal displacement of the containment at different height in case of application of the load-time function (Phantom F4)

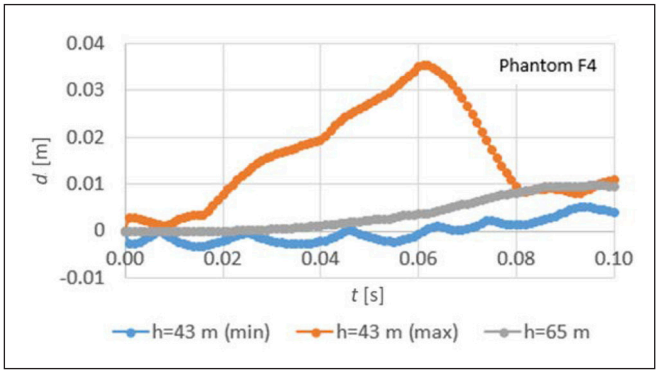

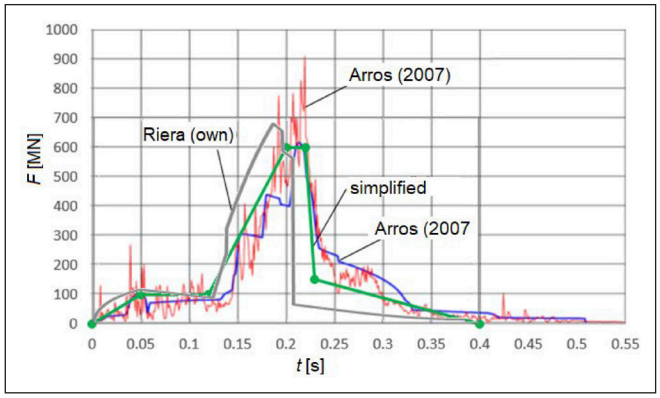

Fig 14: Load-time functions for impact of a Boeing 747 with 215 m/s

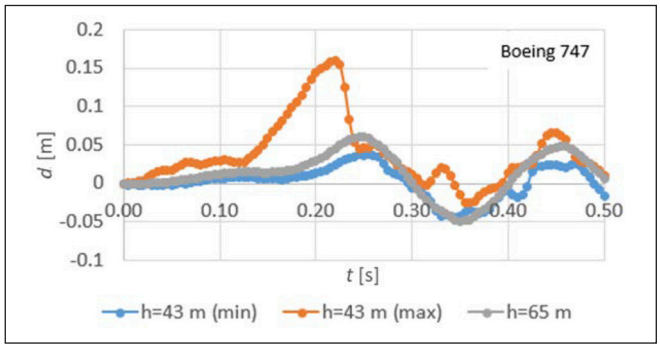

Fig 15: Maximum horizontal displacement of the containment at different height in case of application of the load-time function (Boeing 747)

4.3 Analysis of passenger aircraft impact

Impact of a Boeing 747 passenger aircraft is analysed by a simplified load-time function determined by the Riera method. It is represented in *Fig. 14*, together with the functions used and measured by Arros (2007). Maximum displacements are presented in *Fig. 15*, results belong to the same points as in *Fig. 13* (top of containment, at the height of the impact at the impact zone and at the point farthest from the impact zone). We can see that the maximum displacement at the impact zone is ~0.16 m and the cantilever-like displacement of the building becomes significant (0.06 m at the top and 0.04 cm at the height of the impact). The maximum tensile stress is 58 MPa in the impact zone, but at the bottom of the cylinder, because of the cantilever-like global behaviour 50 MPa tensile stress also arises, therefore in this case crack formation and nonlinear-behaviour should be considered not only at the impact zone but also at the zone close to the support.

5. CONCLUSIONS

In our paper preliminary analysis for aircraft impact into a prestressed concrete containment building was executed, effect of prestress was taken into account by initial conditions of the dynamic analysis. Both missile-target interaction analysis and load-time function method were applied and impact of a Phantom F4 military jet and a Boeing 747 passenger aircraft was examined. Impact of the Phantom F4 caused significant deformations and stresses around the impact zone, where the maximum horizontal displacement was 0.03-0.04 m. In case of the impact of the Boeing 747 aircraft, the maximum displacement was ~0.16 m and global cantilever-like motion of the building was also significant. The analysis showed that application of nonlinear material models and detailed structural modelling are needed around

the impact zone and in case of the Boeing 747 also around the supports, because these are the critical zones where crack formation and nonlinear material behaviour (yielding of steel bars, softening of tensioned concrete, plastic deformations etc.) occur. The results of such preliminary analysis are useful for approximation of the effects and to show the further required steps and level of detailed modelling.

6. ACKNOWLEDGEMENT

The research reported in this paper was supported by the Higher Education Excellence Program of the Ministry of Human Capacities in the frame of the Water sciences & Disaster Prevention research area of the Budapest University of Technology and Economics (BME FIKP-VÍZ).

7. REFERENCES

Annex 3/A to Government Decree No. 118/2011 (VII.11.) http://www.oah.hu/web/v3/HAEAportal.nsf/05F9A474178B5B8CC1257E370029DCE1/$FILE/NSC_3a_en.pdf

Areva (2007), „UK EPR. Fundamental Safety Overview, Vol. 1: Head Document, Chapter A: EPR Design Description"

Arros J. (2007), „Analysis of aircraft impact to concrete structures." *Nuclear Engineering and Desig*n 237, pp. 1241-1249. https://doi.org/10.1016/j.nucengdes.2006.09.044

Asmolov, V. G., Gusev, I. N., Kazanskiy, V. R., Povarov, V. P., Statsurab, D.B. (2017), „New generation first-of-the kind unit – VVER-1200 design features", *Nuclear Energy and Technology* 3 (4), pp. 260-269. https://doi.org/10.1016/j.nucet.2017.10.003

Aszódi A. (2017), „Technical and safety analysis of nuclear power technology." website of Paks 2 NPP. http://www.paks2.hu/en/news/SitePages/newsDetails.aspx?NewsID=241

Aszódi A. (2007), „Why the VVER-1200 techology was chosen by Hungary during the realization of Project Pak II?" (in Hungarian) https://aszodiattila.blog.hu/2017/09/25/miert_a_vver-1200_technologiat_valasztotta_magyarorszag_a_paks_ii_projekt_megvalositasakor

Blinkov, V. N, Melikhov, O. I., Melikhov, V. I.,Davydov, M. V., Wolff, H. and Arndt S. (2012) „Experimental Studies for the VVER-440/213 Bubble Condenser System for Kola NPP at the Integral Test Facility BC V-213" *Science and Technology of Nuclear Installations* Vol. 2012. Article ID 275693. http://dx.doi.org/10.1155/2012/275693

Boros I. (2017), slide of presentation of the subject „Technologies in nuclear power plants- Containment" (in Hungarian), Institution of Nuclear Techniques, Budapest University of Technology and Economics. http://oldweb.reak.bme.hu/fileadmin/user_upload/felhasznalok/boris/AE_Technologiak_VIK/2017_05_AE_Technologiak_BI_kiadott.pdf

Government Decree 118/2011 (2011): https://net.jogtar.hu/jogszabaly?docid=A1100118.KOR

Iqbal, M. A., Rai, S., Sadique, M. R., Bhargava, (2012) „Numerical simulation of aircraft crash on nuclear containment structure." *Nuclear Engineering and Design*. 243, pp. 321-335. https://doi.org/10.1016/j.nucengdes.2011.11.019

Katona, T. (2015), „Design of systems of high significance and their elements. The containment and its systems. Constructional arrangement of the containment and its structural integrity" (in Hungarian) http://oldweb.reak.bme.hu/fileadmin/user_upload/felhasznalok/karolyi/kontenment.pdf

Kennedy, P. (1976), "A review of procedures for the analysis and design of concrete structures to resist missile impact effects." *Nuclear Engineering and Design* 37, pp. 183-203. https://doi.org/10.1016/0029-5493(76)90015-7

Laczák, L.E. (2017) "Evaluation of important parameters of aircraft impact into relatively rigid engineering structures." PhD dissertation, Budapest University of Technology and Economics.

Laczák, L.E. and Gy. Károlyi (2016) "Local Effects of Impact into Concrete Structure." *Periodyca Polytechnica Civil Engineering* 60, pp. 573-582. https://doi.org/10.3311/PPci.8605

Li, Q. M., Reid, S. R., Wen, H. M., Telford, A. R. (2005) "Local impact effects of hard missiles on concrete targets." *International Journal of Impact Engineering* 32, pp. 224-284. https://doi.org/10.1016/j.ijimpeng.2005.04.005

Murthy, A.R.C., Palani, G. S., Iyer, N. R. (2010) "Impact analysis of concrete structural components." *Defense Science Journal* 60, pp. 307-319. https://doi.org/10.14429/dsj.60.358

Riera, J. D. (1968), „On the stress analysis of structures subjected to aircraft impact forces." *Nuclear Engineering and Design* 8, pp. 415-426. https://doi.org/10.1016/0029-5493(68)90039-3

Sahlin et al.: Evaluating the impact of climate change on the risk assessment of Nuclear Power Plants, Safety and Reliability of Complex Engineered Systems – Podofillini et al. (Eds) © 2015 Taylor & Francis Group, London, ISBN 978-1-138-02879-1. https://www.researchgate.net/publication/282504897_Evaluating_the_impact_of_climate_change_on_the_risk_assessment_of_Nuclear_Power_Plants/figures?lo=1

Sandia National Laboratories (2003) „Overpressurization Test of a 1:4-Scale Prestressed Concrete Containment Vessel Model." NUREG/CR-6810, SAND2003-0840P, https://www.nrc.gov/docs/ML0320/ML032040014.pdf

Sugano, T., Tsubota, H., Kasai, Y., Koshika, N., Orui, S., von Riesemann, W. A., Bickel, D. C., Parks, M. B. (1993-1) „Full-scale aircraft impact test for evaluation of impact force." *Nuclear Engineering and Design* 140, pp. 373-385. https://doi.org/10.1016/0029-5493(93)90119-T

Sugano, T., Tsubota, H., Kasai, Y., Koshika, N., Ohnuma, H., von Riesemann, W. A., Bickel, D. C., Parks, M. B. (1993-2) „Local damage to reinforced concrete structures caused by impact of aircraft engine missiles Part 1. Test program, method and results." *Nuclear Engineering and Design* 140, pp. 387-405. https://doi.org/10.1016/0029-5493(93)90120-X

Sugano, T., Tsubota, H., Kasai, Y., Koshika, N., Ohnuma, H., von Riesemann, W. A., Bickel, D. C., Parks, M. B. (1993-3) „Local damage to reinforced concrete structures caused by impact of aircraft engine missiles Part 2. Evaluation of test results." *Nuclear Engineering and Design* 140. https://doi.org/10.1016/0029-5493(93)90121-O

Teland, J. A. (1998), "A review of empirical equations for missile impact effects on concrete. Report no. FFI/RAPPORT-97/05856.", Norwegian Defence Research Establishment, Kjeller.

wikipedia.org, Ohi Nuclear Power Plant, https://en.wikipedia.org/wiki/Ōi_Nuclear_Power_Plant

Wolf, J.P., Bucher, K. M., Skrikerud, P.E (1978), "Response of equipment to aircraft impact." *Nuclear engineering and design* 47, pp. 169-193. https://doi.org/10.1016/0029-5493(78)90014-6

Dr. Lili Eszter Hlavicka-Laczák (1988), civil engineer (MSc), PhD, assistant professor at the Department of Structural Engineering, Budapest University of Technology and Economics. Main fields of interest: analysis of structures under impact and dynamic loads, Member of the Hungarian Group of ***fib.***

Prof. György Farkas (1947) civil engineer (MSc), PhD, Dr. habil, professor emeritus at the Department of Structural Engineering, Budapest University of Technology and Economics. Main fields of interest: construction and design of prestressed concrete structures, Member of the Hungarian Group of ***fib*** and the Hungarian Academy of Engineers.

PREFAB WATER TOWERS FOR LOWER STORAGE CAPACITIES

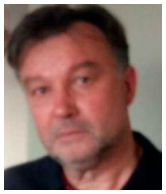


DOI: 10.32970/CS.2019.1.3

Dr. Béla Csíki – Károly Kőszeghy

Due to the recent demand for water supply developments in Hungary two types of water towers made of prefabricated elements have been developed for lower storage capacities, from 50 m³ up to 750 m³. The paper summarizes the design aspects and also the experiences obtained during the construction of five new water towers of various capacities in this range having been realized, so far. Although the application of steel towers in lower storage ranges has been regarded more typical, the realization of prefabricated concrete water towers has proved to be favourable and economic as well.

Keywords: water tower, prefabrication, prestressing, post tensioning, mast, tank, foundation cone.

1. INTRODUCTION

In connection with the recent water supply developments in the country two water tower types have been developed for lower water storage capacities in Hungary. The first type is applicable for 50 m³ to 100 m³, while the second type can be used from 150 m³ up to about 750 m³ storage capacities. Both types are almost fully made of prefabricated reinforced concrete elements. Feasibility of the realization in a storage range frequently covered by steel towers is based on the following – for long time existing – prefabrication capacities of

- circular pipe concrete elements widely used to build underground conduits, and
- wall- and roof elements for prefab under surface circular basins often built for drinking water storage in the past few decades.

The idea of creating water towers by using such prefab reinforced elements was coming from the manufacturer of the elements itself, AGM Beton Zrt. (H-2200 Monor, Külterület, Hrsz.: 0100/8). The company playing an increasing role in the civil engineering execution market in Hungary and abroad was the main contractor of the execution of the five recently built water towers in Hungary, as well.

There are many examples for reinforced concrete water towers built by using prefabricated elements. In most cases the mast is erected monolithically using sliding shutter, while the tank is assembled on the land surface from prefab elements before lifting it up to its final position (Koperniczky, 1969). An alternative method is also widely used: cast in situ concreting of the tank on mounted shutter elements at the bottom surface before moving it up the tower (Kiss and Tóth, 1973). There are much fewer instances for prefabrication extending also to the mast of the water tower. An interesting example is a set of uniform 200 m³ water towers of such a kind in Italy, near Verona (Márkus, 1984). In addition to the tank also the mast of the towers was made of prefabricated elements connected by prestressing (post-tensioning). Mainly the mast prefabrication resulted in a very short (3 weeks/tower) building time of these towers often commemorated about. The present paper on the issue is a re-edited version of a CCC congress presentation held in Hungary (Csíki, et al., 2017).

2. STRUCTURAL ARRANGEMENT

2.1 Tower shaping

Shaping of both tower types are based on putting together prefab pipe-, wall- and roof elements in order to get the superstructure - the mast and the tank, as well - of a water tower. The mast of both water tower types is made of vertically post-tensioned prefabricated reinforced concrete pipe elements. The storage tanks above the mast are also fully prefabricated with watertight connections, but the arrangements are slightly different.

The design view and the vertical section of tower Type 1. for lower (from 50 to 100 m³) capacities is shown in Fig.1.

Tower Type 2.is developed for a bit higher (from 150 to 750 m³) storage capacities, Fig.2.

The circular tank-wall of the first type for smaller capacities consists of cylindrical segment elements. The tank-wall of the second type for the bigger capacity is polygonal in layout, and consists of vertical plain panels. The only main structural part of both types made of in-situ reinforced concrete is the founding of the water-towers.

2.2 Substructure and foundation

The substructure consisting of a foundation slab and of a founding cone at both water tower types is made of in-situ (monolithic) reinforced concrete.

Depending on the soil conditions of the site plane- or piled foundation is applied. The foundation method determines the necessary layout measure of the applied (circular or polygonal) foundation slab. (A piled foundation may need less size in layout.)

The founding cone stiffening the substructure on the one hand secures the entrance of the tower, on the other hand serves

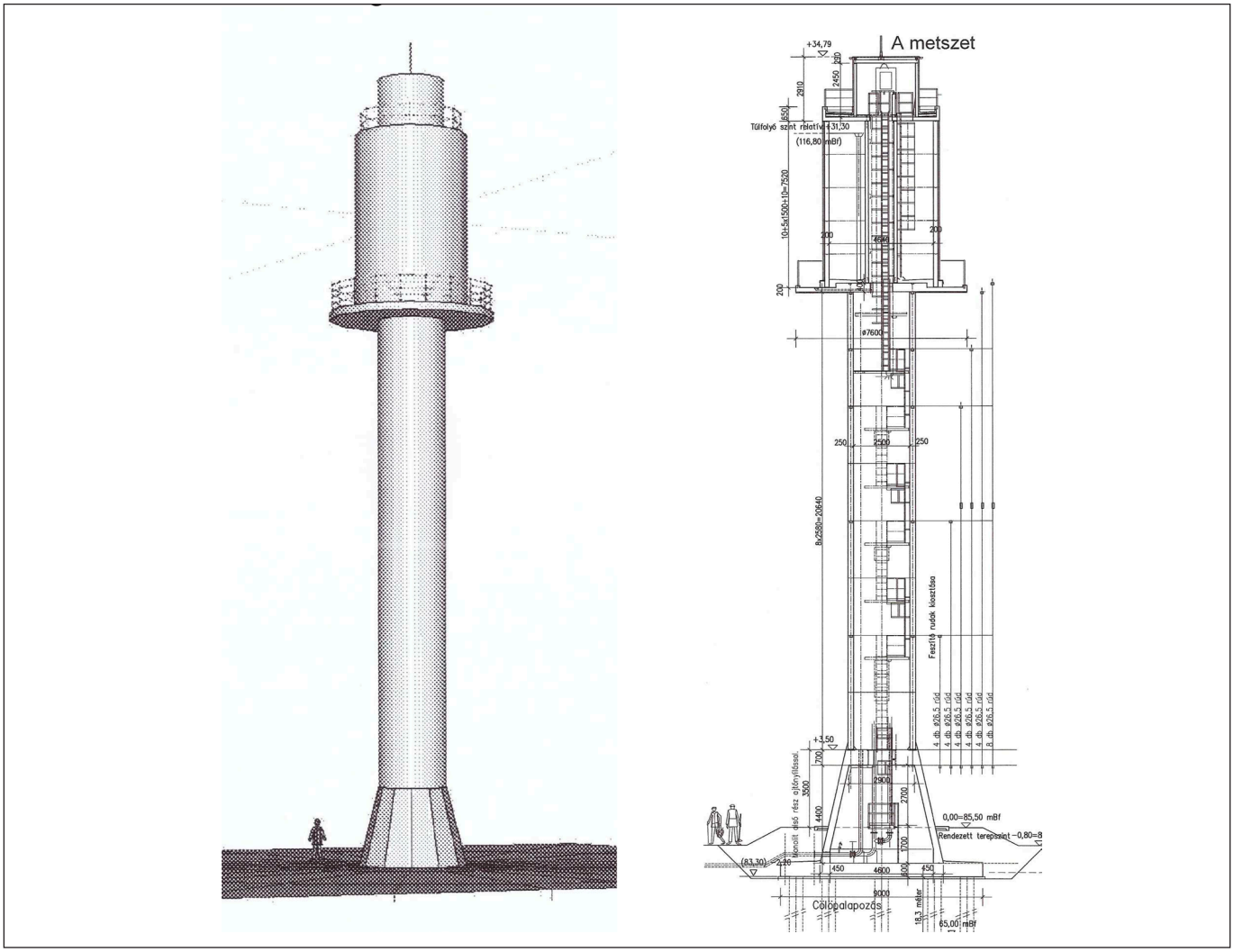

Fig. 1. *Design view and section of tower Type 1*

as anchoring space for the prestressing bars of the mast. The height of the cone is about 5 m, the diameter is changing from 3 m to 5 m. The thickness of the roof slab of the cone where the mast prestressing bars are fixed to is 0.7 m.

The applied grade of structural concrete for the substructure is C35/45-XC4-XF1-XA1, with a reinforcing steel category of B500B.

2.3 Prestressed mast

The mast of both tower types consists of prefabricated reinforced concrete pipe elements of 3.0 m outer diameter and of 250 mm wall thickness. The height of the pipe elements is 2.58 m. The number of the mast elements can be about 9 to 11 pieces depending on the required tower height. At tower Type 2 the last element is special to allow for anchoring radial cantilever beams directly supporting the tank.

The mast elements are gradually post-tensioned through the pipe-walls in vertical direction by prestressing bars anchored at the bottom of the thick roof of the founding cone. In the realized cases Dywidag prestressing bars (DSI 950/1050) of 26.5 and 32 mm diameter were used.

The applied grade of structural concrete for the mast elements is C50/60-XC4-XF1-16-F3, with reinforcing bars of B500B.

2.4 Tank supporting

The direct supporting of the tank at the top of the mast is different for the two tower types.

At Type 1. an in-situ prefabricated reinforced concrete circular plate is lifted and fixed directly to the final mast element. Then, the prefab segment elements of the tank are placed directly to the circular plate functioning as bottom plate of the tank.

At Type 2. radially located, reinforced concrete cantilever beams are used for supporting the tank. The bottom plate is made of in-situ reinforced concrete casting on prefabricated shallow shutter slabs after they have been lifted up to the cantilevers. Fixing and anchoring of the radial prefabricated cantilevers to the specially arranged, final mast element was one of the most challenging questions to be solved during the design, Fig. 3.

2.5 Tank structures

The storage tanks above the mast are also fully prefabricated with watertight connections, but the arrangements of the sidewalls are slightly different, Fig.4. The effective layout of tanks for water storage is circular ring-shaped (not circle) because of a central circular pipe-element with a steel ladder inside connecting the mast area with the tank-roof to secure free access. This central pipe acts as an inner support of the tank-roof, as well.

The circular tank-wall of Type 1. for smaller capacities consists of prefabricated cylindrical segment elements of 200 mm thickness, and of 1.50 m height connected to form whole circles (rings) at the ground surface. Each ring including three connected segments is lifted up to the bottom plate on the mast

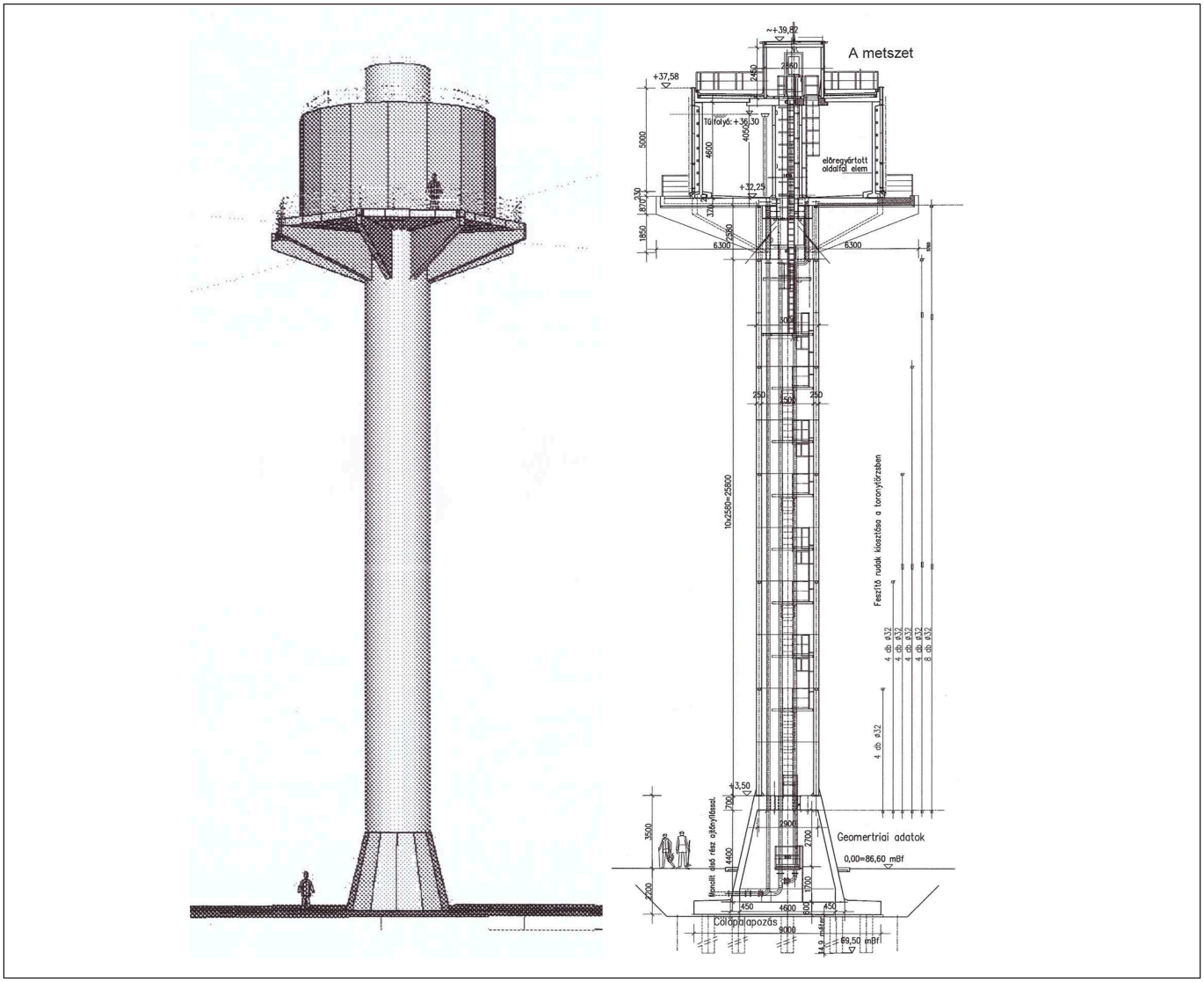

Fig. 2. *Design view and section of tower Type 2.*

(or onto the previous full ring). A 100 m^3 capacity tank is of 4.64 m diameter, with a 7.50 m necessary wall height. This height can be reached by five whole rings with four circumferential watertight connections worked up at their final location by special sticking material and welding.

The tank-wall of Type 2. for the bigger capacity is polygonal in layout. It consists of prefabricated vertical plain panels with horizontal and vertical stiffening ribs at the panel-edges. The panels are connected to each-other by bolts along the vertical ribs, while their bottom is welded to steel continuous profiles concreted in the bottom plate. The water-tightness at each junction is secured by cement-slurry injection of the designed gaps.

Regarding a 200 m^3 storage capacity tank, 16 wall-panels of 1.76 m width are needed, arranged around a 9.16 m diameter inner circle of the 16 sides polygon. The height of the panels is 4.60 m, with lowest thickness of 150 mm. (Tanks of similar arrangement with several measures were widely used in Hungary to build underground water reservoirs a few decades ago.)

The grade of structural concrete to the prefab elements of the water tanks is C40/50-XV2(H)-XC2-XD2. The category of the applied reinforcing steel is B500B.

Fig. 3. *Anchoring of radial cantilevers to the final mast element (Type 2.)*

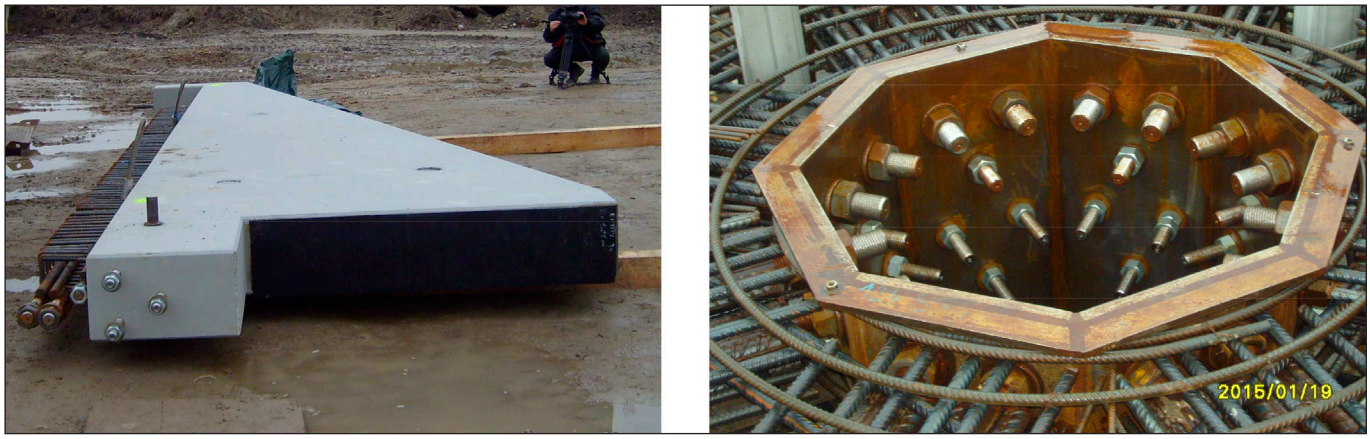

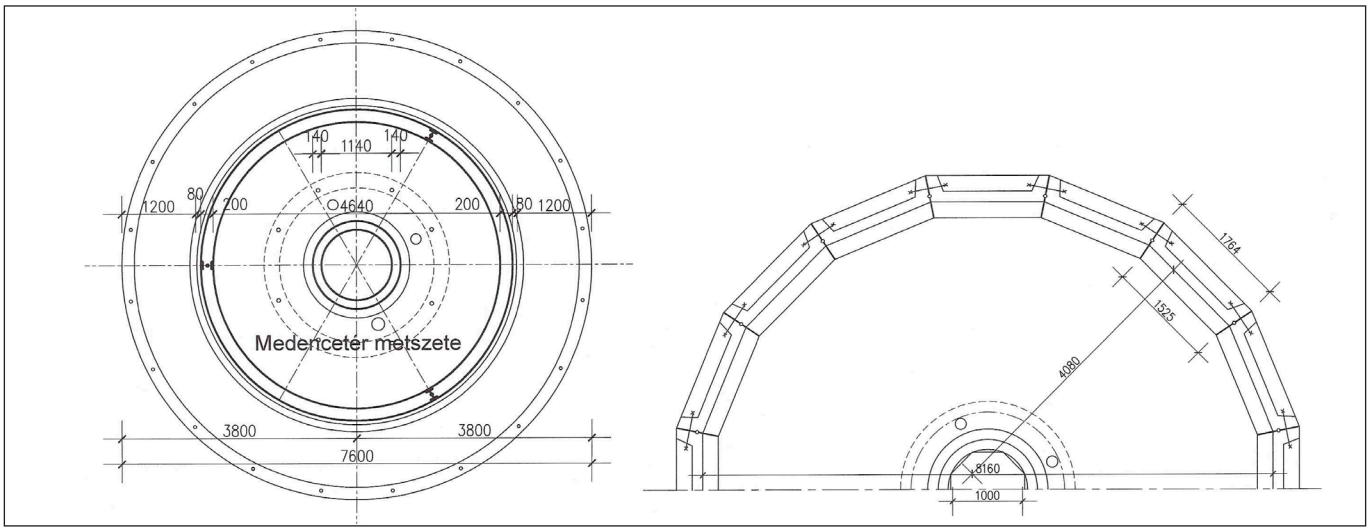

Fig. 4. Tank horizontal sections (Type 1 left, Type 2 right)

2.6 Mast and tank element joints

The circular horizontal joints of the mast elements are formed by smooth surfaces (without any notches) compacted by sticking and – obviously – by the prestressing itself.

The watertight joints of tank elements of both Types at the bottom slab are formed by mixing of in-situ welding and concreting. The wall to wall circumferential joints at tank of Type 1. are notched connections compacted by sticking and welding. The vertical joints along the wall elements of Type 2. are bolted and in-situ cement injected connections.

3. STRUCTURAL ANALYSIS

The following structural models, design principles and analysis methods were applied to the structural design of the water towers:

- *In general:*

Three-dimensional combined structural model on elastic bedding or on discrete elastic springs examined by FEM (Fig. 5).

- *To earthquake load* (Modal response spectrum analysis):
  1. Static model: Reduced at the mass centre (one mass) vertical cantilever. The water load (weight) is considered in the metacentre when determining the mass centre.
  2. Dynamic model: Two mass (M1, M2) vertical cantilever. M1 is the sum of the mass of the tower and of the mass of the impulsive water part (moving together with the structure) acting in the mass centre. M2 is the mass of convective water part (moving separately from the structure) suspended in the metacentre.
- *To stability analysis:*

Elastically supported (walled in) vertical cantilever. (The critical force based on *Föppl-Papkovics* principle.)

- *Prestressing of the mast:*

The effective (applied in two steps) prestressing forces of the mast are increasing from top to bottom to eliminate tension stresses along the mast. The distribution of the considered prestressing forces and of the normal forces due to an ultimate load combination of 200 m^3 water tower in Gádoros (Hungary) is presented in Fig. 5.

Fig. 5. FEM model of structure, Prestressing- and axial forces of mast

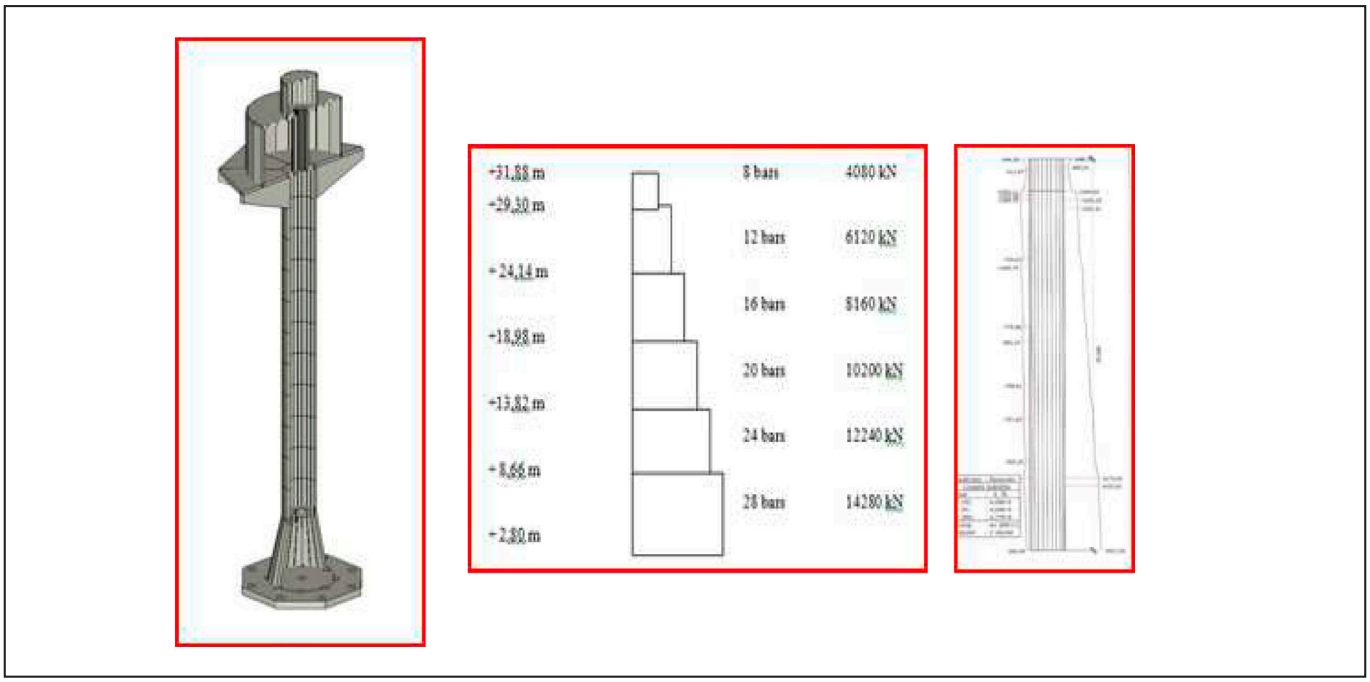

Fig. 6. Examples for mounting-like construction (Type 2)

4. CONSTRUCTION ASPECTS, FEASIBILITY OF APPLICATION

To satisfy a recent demand for high water storage of lower range capacity, five new type almost fully prefabricated reinforced concrete water towers have already been built, in Hungary. Three of the first type with 100 m^3 storage capacity were built and put in operation in Árpádhalom, Eperjes and Újiráz in 2015. Two of the second type have been built so far: one of 200 m^3 capacity in Gádoros in 2015, and one of 500 m^3 capacity in Dömsöd in 2014.

The prefabrication of the elements and the leading of the in situ construction works for all the new towers were done by AGM Beton Zrt. (H-2200 Monor, Külterület, Hrsz.: 0100/8, Hungary). Advantages regarding the construction time and cost effectiveness of building almost fully prefabricated reinforced concrete towers have proved to be considerable because of the following reasons:

- There has been, for long time, a prefabrication capacity for reinforced concrete elements applicable (by not much modification) to build mast and tank of water towers.
- There have been, for long time, building experiences of prefabricated water reservoirs on or under the ground.
- The mounting-like building activity needs low living labour capacity (Fig. 6).
- Possibility of more tower construction at the same time with not multiple recourses. This may reduce multiple costs.
- Possibility of very short building time. After the in-situ concreting works of the substructure have been done the building time of mounting is not more than a few weeks.

5. CONCLUSIONS

Two types of water towers almost fully made of prefabricated elements have been developed for lower ranges of water storage capacity, recently. The first can be used for 50 m^3 to 100 m^3, while the second type is applicable from 150 m^3 up to 750 m^3 storage capacities. The design aspects and also the experiences obtained during the recent erection of five new type water towers have been summarized in the paper.

Realization of the water towers proved to be economic due to the short time of in-situ building works and also to the (for long time) existing prefabrication capacity. The experiences have been positive so far regarding the operation aspects of the towers as well.

Hopefully, the new civil engineering structures, as special kinds of landmarks, satisfy the aesthetic considerations, as well, Fig.7.

6. ACKNOWLEDGEMENTS

The authors must express their thanks to AGM Beton Zrt. (H-2200 Monor, Külterület, Hrsz.:

0100/8, Hungary), the general contractor of the towers for the possibility of taking part in the development and design of the new type civil engineering structures.

Fig. 7. Views of the water tower types (Type 1 left, Type 2 right)

Special thanks to Gábor Szilágyi, general manager of the company and to his colleagues, who were taking part in the detailing of the structural design.

7. REFERENCES

Csíki, B., Kőszeghy, K., Perczel, Z. (2017), "New Type Prefabricated Water Towers with Prestressed Mast", *Proceedings of CCC 2017*, Tokaj, Hungary, September 2017, pp. 15-22.

Kiss, I., Tóth, L. (1973), "Water tower of Balaton Youth-town", *Műszaki Tervezés*, (in Hungarian) March 1973, pp. 27-29.

Koperniczky, J. (1969), "Construction of small water towers", *Műszaki Tervezés*, (in Hungarian) March 1969, pp. 19-22.

Márkus, G. (1984), "Reinforced concrete reservoirs", *Mérnöki Kézikönyv, II.,* (in Hungarian) 1984, pp. 920-942.

Dr. Béla CSÍKI (1957), MSc (1982), Doctorate (1993), Civil Eng., TU Budapest. MSc Real Estate (2002), NTU Nottingham. Employments: DCB Engineering Ltd., managing director (2003-), E&H Ltd., technical director (2016-). He is a member of the editorial board. His main field of interest is dealing with specific structural problems of and also the design of special civil engineering structures mainly in connection with water and waste water treatment or industrial fields. He has been author of several papers on his professional activity.

Károly KŐSZEGHY (1944), MSc (1970), Civil Eng., TU Budapest. From 1970 he worked for more than two decades for company named Mélyépterv dealing with and leading the design of substantial civil and structural engineering structures at the time. Since 1993 he has been working for his own company, Kőszeghy Ltd. His professional work covers several fields of structural engineering in Hungary and abroad, such as: developments in prefabrication for civil engineering, design of special structures, sludge digesters, reservoirs, towers, industrial buildings, etc. Several studies and papers commemorate his specialties.

THE EFFECT OF AGE AND TESTING METHOD ON THE ADDED FRACTURE ENERGY OF FIBRE REINFORCED CONCRETE


Károly Péter Juhász – Péter Schaul

DOI: 10.32970/CS.2019.1.4

The use of Fibre Reinforced Concrete (FRC) is widely accepted in the tunnelling industry. The generally accepted method to determine the material parameters of FRC is the standard 3-point beam test. The effect of age can be relevant for tunnels, because these structures are usually designed for life cycles over 100 years. In this paper the test results of FRC specimens with different fibres using different testing methods (beam and square panel) at different ages will be presented. FRC changes its properties over time in case of both fibre types. The post crack capacity of steel FRC increases in beam tests, while it decreases in panel tests, which yields the conclusion that steel fibres work better at smaller crack width. This changes only a small amount over time. The energy absorption measured from panel tests reduces in case of steel fibre, but stays at a constant level for synthetic fibre.

Keywords: fibre reinforced concrete, testing age, panel test, beam test

1. INTRODUCTION

Fibre reinforced concrete has been widely used over recent decades in the tunnelling industry, in infrastructural structures like tramlines, railway track slabs and in industrial floors for instance, primarily due to its main advantage of increasing the ductility of the quasi-brittle concrete while providing a post-cracking strength to the composite material (Juhász, 2014). There are several raw material sources for these fibres, but the two main types are steel and macro synthetic fibres. Steel fibres usually have hooked ends and macro synthetic fibres typically have a fully embossed surface. The interaction between these fibres and the concrete matrix can define the properties of the fibre reinforced concrete material. Under loading the addition of fibres in the concrete can bridge the crack sides, but after reaching a critical load level they will fail either in rupture or in pull out (Zollo, 1997). The best residual strength capacity can be obtained when the bond strength of the fibres is high and where the fibres are not rupturing. To reach this performance, highly engineered fibres are needed where both the tensile strength of the fibres and the pull-out resistance of the fibres are high. To increase the pull-out resistance multiple hooks can be used in the case of steel fibres, while in the case of macro synthetic fibres the embossing on the surface plays a key role in pull-out resistance. However, the chemical treatment of the surface (sizing) is also a very important factor. Over time the bond between the fibres and the concrete matrix can change, which can lead to an unfavourable behaviour of the composite material. It can happen that the bond strength of the matrix becomes too strong over time and the composite exhibits brittle fibre rupture instead of ductile pull-out behaviour. This phenomenon is called embrittlement in recent literature (Bernard, 2008). Over time the bond strength can also decrease, which in turn leads to a similar loss of post-crack performance.

In this paper the results of experimental investigations on panel and beam specimens reinforced with steel and macro synthetic fibre at different test ages will be presented and discussed.

2. CORRELATION BETWEEN THE BOND STRENGTH AND THOUGHNESS

The pull-out phenomenon of fibres in fibre reinforced concretes was investigated by Bartos (1980, 1981). According to his study the failure mode of the composite depends on the length and the tensile strength of the fibres. With regard to the fibre length the failure mode can be a sudden de-bonding or a progressive de-bonding. Regarding the strength of the fibres, the failure mode can be pull-out or rupturing. The fibre is optimal if it can maximally increase the ductility of the composite material. According to Kelly (1973), maximum ductility can be achieved when the bond strength of the fibres is equal to τ_c, which is the critical bond value. If the bond strength is less than this value the fibres will pull out from the concrete matrix, if it is larger the fibres will rupture and the ductility will decrease (Figure 1).

Figure 1. Pull-out work and interfacial bond strength (Kelly, 1973)

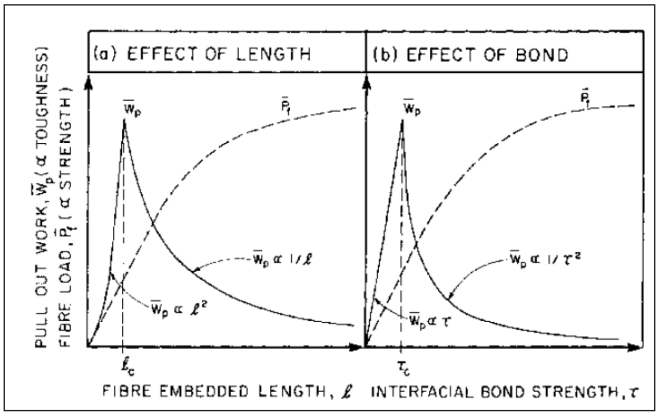

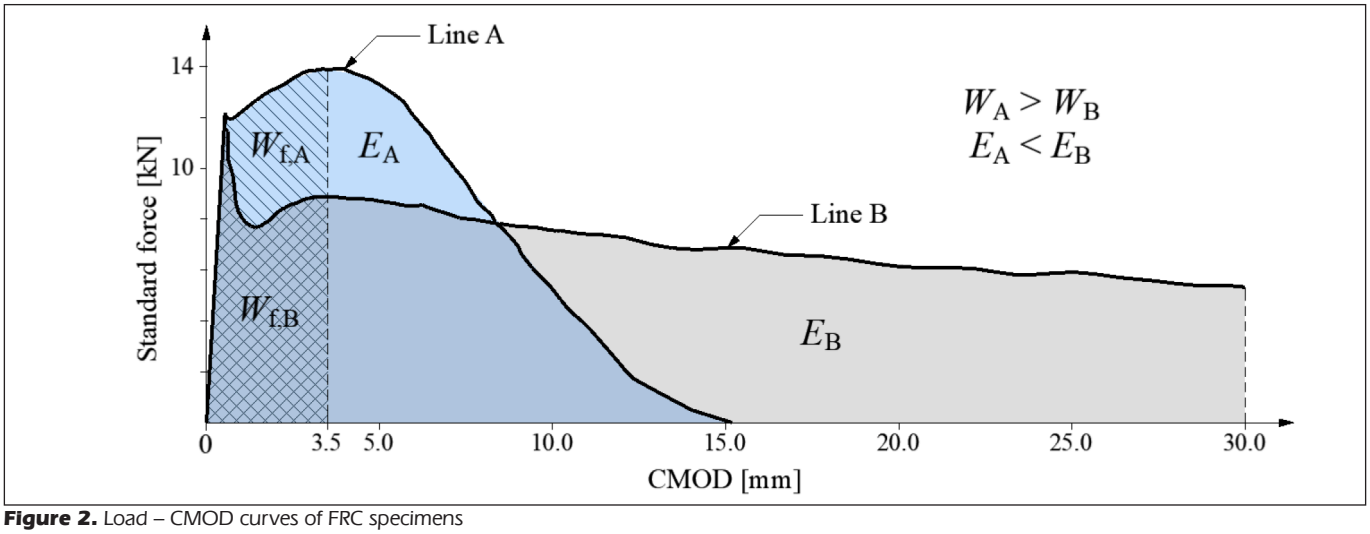

Figure 2. Load – CMOD curves of FRC specimens

The most common way to examine fibre reinforced concrete properties is the three point bending beam test according to the European harmonised standard EN 14651:2005 by measuring the applied load versus the constantly increasing Crack Mouth Opening Displacement (CMOD). The maximum value of the CMOD is 3.5 mm in these tests, i.e. the fibres are not necessarily pulling-out from the concrete matrix and thus their effect on the ductility cannot be fully investigated.

Figure 2 shows the Load-CMOD diagrams of two fibre reinforced concrete specimens out to a displacement of 30 mm. One of the fibres has a high pull-out resistance, which is limited to small crack widths only, while the other one has a lower initial pull-out resistance, but it is not significantly decreasing even at wider cracks. The 3.5 mm CMOD value is marked in the figure, representing the standard limit of the beam test.

These diagrams represent well the characteristic behaviour of steel fibre and macro synthetic fibre reinforced concrete specimens. While the steel fibres are working well at small crack widths, they lose efficiency dramatically with increasing crack width (line A). On the contrary, macro synthetic fibres exhibit constant pull-out resistance, even at much wider cracks, due to the different energy absorption characteristic (line B) (Juhász, 2013; Bernard, 2009). This difference can be clearly seen in those tests where the maximum crack width or deflection values are larger than the mentioned 3.5 mm, for example in case of square panel tests according to EN 14488-5:2006. In such a testing configuration, the difference is much larger and in addition, the absorbed energy characteristic will change, i.e. the energy absorption capacity of the macro synthetic fibres will be greater than the capacity provided by steel fibres.

The area under the Load-CMOD diagram of a beam test is referred to as "fibre-work" (Tóth, Juhász, Pluzsik, 2017), where the area under the load-displacement curve of a square panel test is referred to as "energy absorption" (see Figure 5). These two parameters represent very well the ductility and the post crack performance of fibre reinforced concrete specimens.

The interaction between the fibres and the concrete matrix is very important, but due to ageing of the surrounding concrete several chemical-physical effects can occur, which have an influence on the bond performance. In "figure 1" it can be seen that the bond strength is a highly sensitive element in the performance of fibre reinforced concrete, whether increasing or decreasing, it can cause a significant change in the ductility of the composite.

3. EXPERIMENTAL INVESTIGATIONS

Steel and macro synthetic fibre reinforced concrete beam and square panel specimens were cast and tested at the Czakó Adolf Laboratory of the Budapest University of Technology and Economics. The objective of this research was to investigate the performance of different fibre reinforced concrete specimen types with increasing age. Specimens were tested at 28 days, 90 days and one year of age.

The concrete mix design was identical in all cases, which was a typical shotcrete mix according to Table 1

Table 1. Concrete mix design

Component	Type	[kg/m3]
Cement	CEM I 42.5 R	480
Water content		216
Aggregate 0/8		1620
Superplasticizer	Mapei Dynamon SXN	4
Fibres	Macro synthetic and steel	6 & 8, 55
w/c	0.45	

To investigate the performance of different fibres one steel fibre and three types of synthetic fibres were used in the test with different dosages. The types of the fibres and their main parameters can be seen in Table 2.

In all cases three square panels and seven beams were cast. To measure the compressive strength of the concrete with every fibre dosage three cubes were also cast. The compressive strength of the concrete was C50/60 according to Eurocode 2. The concrete was mixed with a Collomix –XM2 - 650 professional mixer. The slump of the concrete was 210 mm and the air content was 6% (Figure 3).

In all cases the fibre mixing was good with the stated dosages, the fresh fibre reinforced concrete was homogeneous and well compacted. The square panels were poured into

Figure 3. Air content and slump test

Table 2. Fibre types and properties

Reference	Fibre name	Fibre type	Fibre dosage	Fibre length	surface/end
BC48-6kg	BarChip48	Macro synthetic	6 kg/m3	48 mm	embossed
BC48-8kg	BarChip48	Macro synthetic	8 kg/m3	48 mm	embossed
BC54-6kg	BarChip54	Macro synthetic	6 kg/m3	54 mm	embossed
BC54-8kg	BarChip54	Macro synthetic	8 kg/m3	54 mm	embossed
DT57-6kg	DucTil57	Macro synthetic	6 kg/m3	57 mm	embossed
DT57-8kg	DucTil57	Macro synthetic	8 kg/m3	57 mm	embossed
SF35-55kg	SF35	Steel	55 kg/m3	35 mm	hooked

Table 3. Test matrix

Reference	28 days		90 days		1 year	
	Beams	Panels	Beams	Panels	Beams	Panels
BC48-6kg	7	3	-	-	-	-
BC48-8kg	7	3	7	-	7	-
BC54-6kg	7	3	-	-	-	-
BC54-8kg	7	3	7	3	7	3
DT57-6kg	7	3	-	-	-	-
DT57-8kg	7	3	-	3	7	3
SF35-55kg	7	3	7	3	7	3

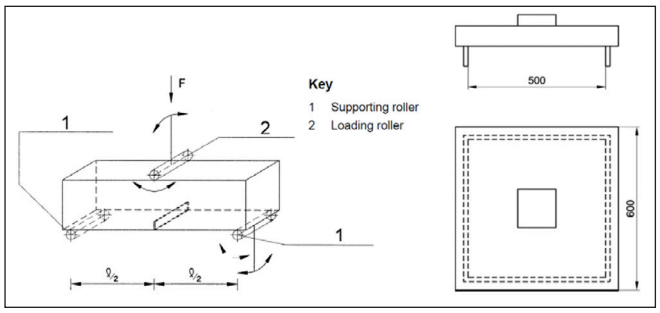

Figure 4. Test supports and arrangement (left: beam test, right: panel test)

the formwork without any vibration, while the beams were compacted on a high frequency shaking table. All specimens were stored underwater at room temperature until tested.

The full test matrix with the testing ages can be seen in Table 3.

The beam tests were conducted according to EN 14651:2005 and the panel tests according to EN 14488-5:2006. In both cases the testing machine was a deflection controlled universal testing machine type Zwick Z150.

In case of the beam tests the speed of the crack mouth opening displacement was 0.05 mm/min until CMOD = 0.1 mm, after that the speed was 0.2 mm/min. In case of the square panel tests the speed of the centre displacement was 1 mm/min. The load-displacement curve was recorded and the test was continued until a deflection of at least 30 mm was achieved at the centre point of the slab. The supports and loading devices of the beams and panels can be seen in Figure 4.

4. TEST RESULTS

The "fibre work" of the beams and the "energy absorption" of the square panels can be seen in Figures 5a and 5b.

In the case of steel fibres the ductility decreased continuously with increasing testing age. According to Kelly (1973) (Figure 1) the bond strength is unknown but the decreasing ductility can be due to two reasons: the bond strength decreased and thus the pull-out resistance also decreased or the bond strength exceeds the critical value and the energy absorption of the fibre changed or the fibres rupture instead of pulling-out. On checking the cracked surfaces, it was found that none of the fibres were ruptured. The loss of ductility is a well-researched topic in case of steel fibre reinforced concrete (Bernard, 2009) who relates this embrittlement effect with the rupture of the fibres due to the increased chemical-physical bond. According to the results it can be seen that the decrease in the bond strength can also decrease the ductility of the fibre reinforced concrete specimens.

In case of synthetic fibre reinforced specimens, the ductility increased or remained constant over the test period. According to Kelly this can be because of the increasing or the decreasing of the bond strength. The number of the ruptured fibres on the cracked cross section was not higher after one year than after 28 days which means that the bond strength increased during the ageing process but it did not reach the critical value.

From the beam test results, it can be seen that the beam test does not represent very well the real fibre performance during the ageing process due to the low level of the deformation and crack widths. Thus, it is questionable whether testing of beams at 28 days of age alone yields sufficient information with regard to the design values obtained hereof and with regard to the design life of the structure.

5. CONCLUSIONS

By adding fibres to plain concrete, the ductility and the post crack performance increases. The bond interaction between the concrete and the fibres is a very important parameter in the case of ductility but it highly depends on the age of the material. With an optimal anchorage length the bond strength can change during the ageing process which can lead to both an increase and a decrease in ductility.

Steel and synthetic fibre reinforced concrete beams and square panel tests were carried out at different ages. While the performance of steel fibre was better in case of beam tests, the energy absorption was superior with synthetic fibres. During the test period the ductility of steel fibres decreased while most of the synthetic fibres' ductility increased or remained constant. On the cracked surface of the steel fibre reinforced concrete specimens none of the fibres were ruptured, which means that the bond strength decreased during the test period. In the case

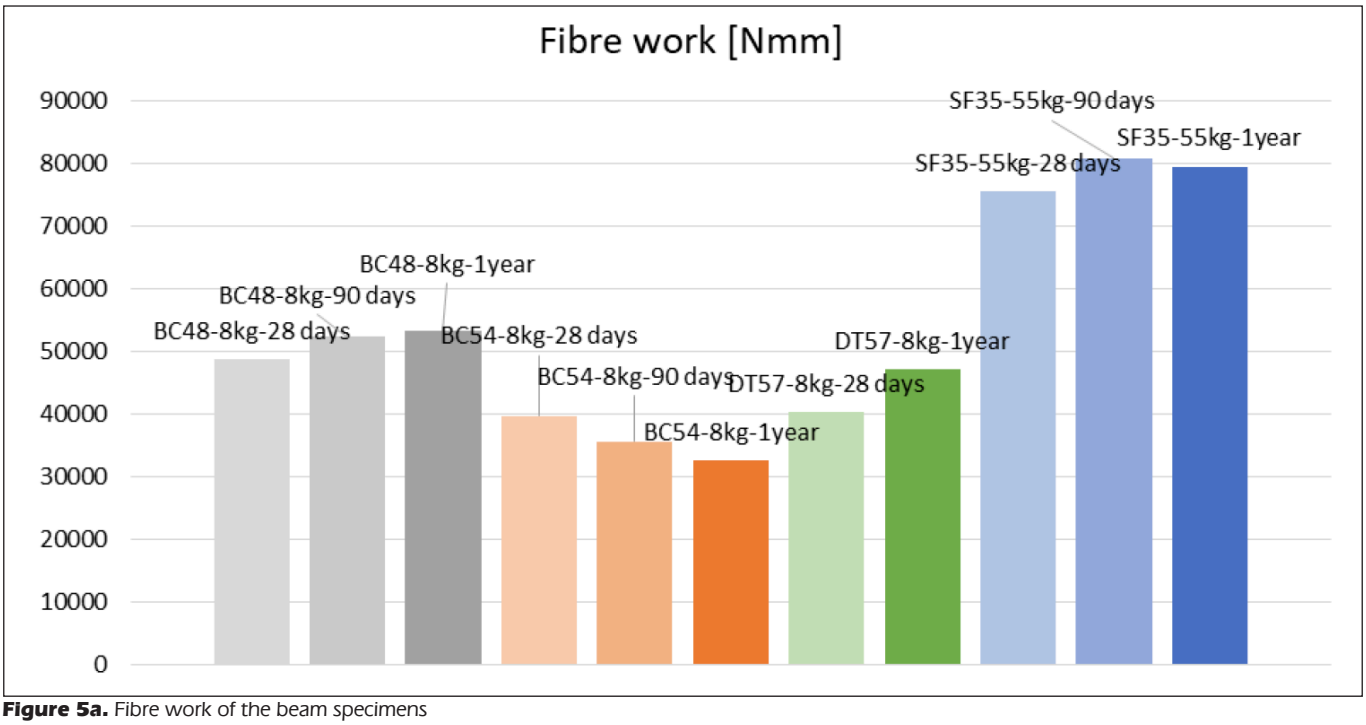

Figure 5a. Fibre work of the beam specimens

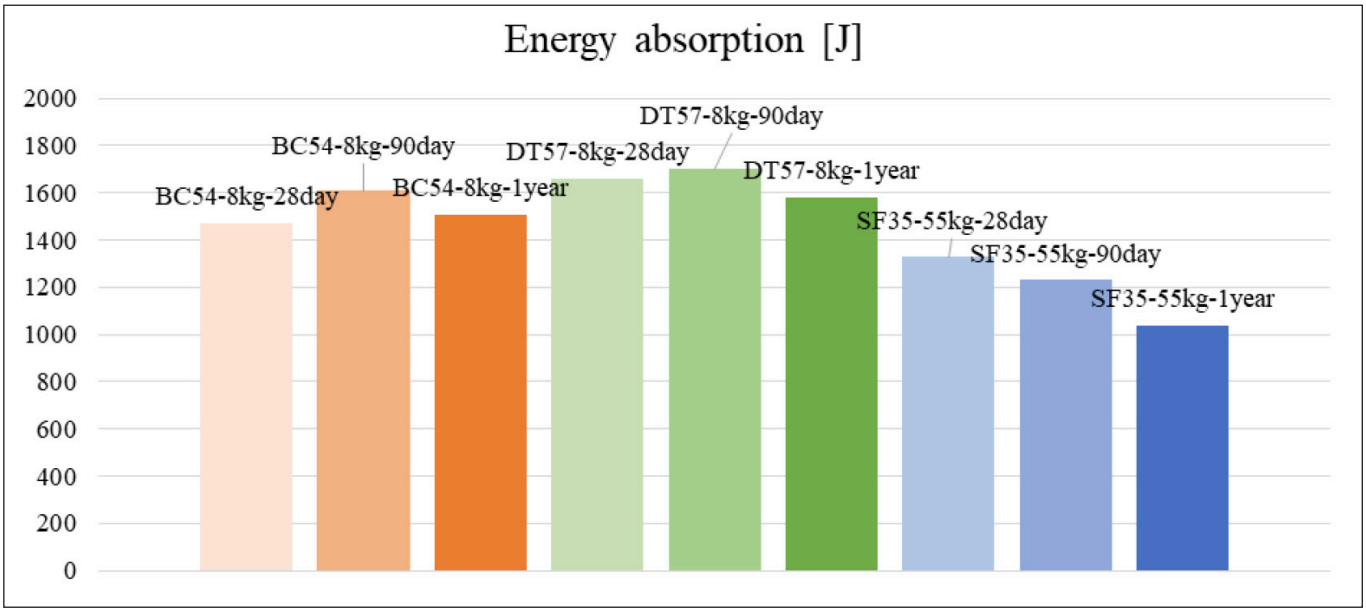

Figure 5b. Energy absorption of the square elements

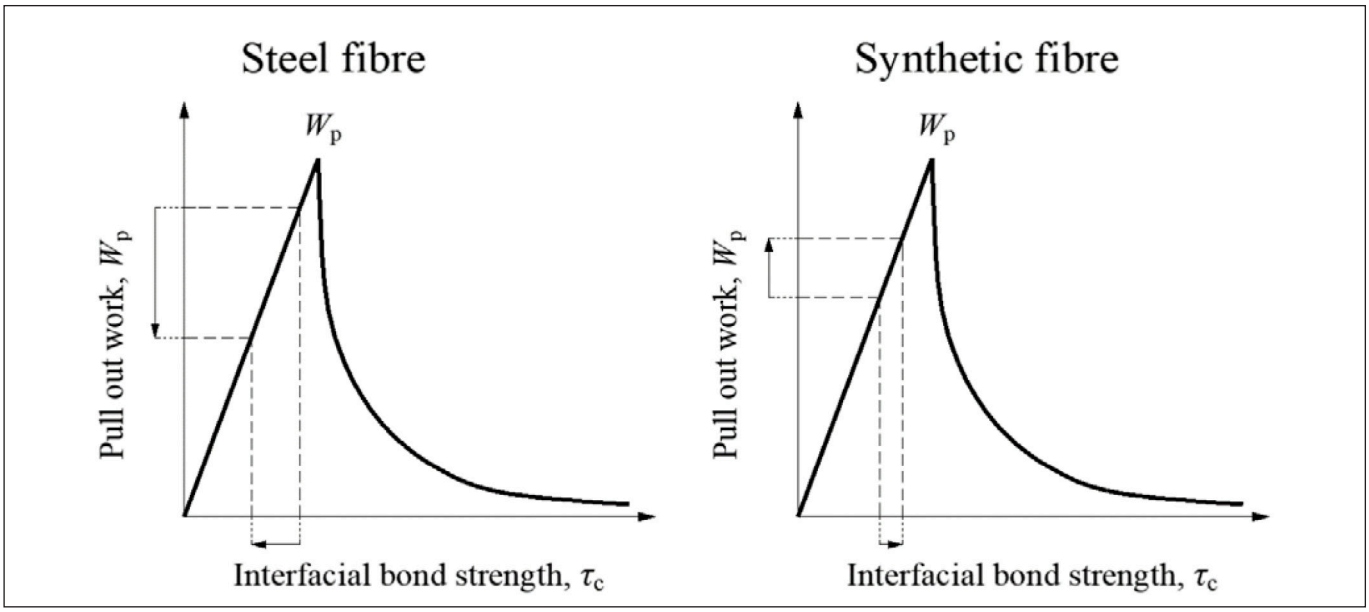

Figure 6. Interfacial bond during ages

of synthetic fibres, the number of the ruptured fibres was not larger over the test period, the bond strength in those cases increased (Figure 6).

Panel tests better represent the ductility of fibre reinforced concrete specimens, the beam test does not represent the real fibre concrete composite performance during the ageing process due to the low level of displacement and crack width.

6. REFERENCES

Bartos, P. (1981). Review paper: bond in fibre reinforced cements and concretes. Interna*tional Journal of Cement Composites & Lightweight Concrete* 3, pp. 159-177.

Bartos, P. (1980). Analysis of pull-out tests on fibres embedded in brittle matrices. *Journal of Material Science* 15, pp. 3122–3128.

Bernard, E. S. (2008). Embrittlement of fiber-reinforced shotcrete. *Shotcrete*, 10 (3), pp. 16-21.

Bernard, E. S. (2009). Design of fibre reinforced shotcrete linings with macro-synthetic fibres. In: *Shotcrete for Underground Support XI, ECI Symposium Series*, P11. (Accessed 15 June, 2013) Retrieved from: http://dc.engconfintl.org/shotcrete/14

Juhász, K. P. (2013). Modified fracture energy method for fibre reinforced concrete. In: A. Kohoutková et al., (eds.) *Proceedings of Fibre Concrete 2013: Technology, Design, Application*. Prague: Czech Republic, pp. 89-90.

Juhász, K. P. (2014). Szintetikus makro szálerősítésű betonok (Synthetic macro fibre reinforced concrete, in Hungarian*). Postgraduate Degree in Concrete Technology, master thesis. Budapest University of Technology and Economics, Budapest.*

Kelly, A. (1973). Strong Solids. Oxford University Press: Oxford.

Tóth, M., Juhász, K. P., Pluzsik, A. (2017). Effect of mixed fibers on the ductility of concrete. *Journal of Materials in Civil Engineering*, Vol. 29, No. 9.

Zollo, R.F. (1997). Fibre-reinforced concrete: an overview after 30 years of development. *Cement Concrete Composites*, 19 (2), pp. 107-122.

Károly Péter Juhász (1980), Structural Engineer MSc., Head of the Czakó Adolf Laboratory, Department of Mechanics, Materials & Structures, Budapest University of Technology and Economics. His main fields of activities are experimental investigation and modelling of synthetic fibre reinforced concrete, finite element modelling of concrete structures. Owner and chief engineer of JKP Static Ltd. Member of the ***fib*** working group 2.4.2.

Péter Schaul (1989), Civil Engineer MSc., PhD student (Department of Construction Materials and Technologies, Budapest University of Technology and Economics). His main fields of activities are experimental investigation and modelling of FRC and FRP structures, finite element modelling of concrete structures. Structural engineer at JKP Static Ltd. Member of the ***fib***.

ÉMI-TÜV

Add value.
Inspire trust.

ÉMI-TÜV SÜD

Solutions that ensure quality, safety and sustainability for future generations

ÉMI-TÜV SÜD is a premium quality, safety and technical service provider that specializes in testing, inspection, auditing, certification, training and knowledge services.

Services of ÉMI-TÜV SÜD:

- Lifts, escalators and moving walks
- Cranes and machinery
- Pressure equipment (boilers, pressure vessels, industrial hose pipes)
- Industrial equipment's and welding technology
- Civil and Structural Engineering Services
- Full-scale testing of structures, elevators and construction products
- Recreational Facilities, Amusement Rides
- Children's Playgrounds & Equipment
- Consumer products (Textiles; Toys and child-care products; Cosmetics, Food and food contact materials; Household products and household chemicals; Paints, varnishes and coatings; Furniture and wood products; Cementitious adhesives; Boilers and fireplaces
- Audit and Management system certification

Our services for the construction industry:

- Technical inspection of existing plants, buildings
- Building Diagnostics
- Assessment of existing structures
- Design and evaluation of structural strengthening
- Testing of load-bearing elements
- Dynamic on-field and laboratory tests
- Compliance checks in accordance with EN standards
- Factory Production Control
- 3rd-Party supervision of construction

ÉMI-TÜV SÜD Kft. 2000 Szentendre, Dózsa György út 26.
(+36) 26 501-120 info@emi-tuv.hu www.emi-tuv.hu

TÜV®

CREATING THE FUTURE

A-HÍD

A-HÍD ZRt.
H-1138 BUDAPEST
KARIKÁS FRIGYES U. 20.

www.ahid.hu